ARTICLE

Moringa oleifera compounds from seeds and extracts from leaves: anticancer and cancer chemopreventive properties; preparation of leaf extract-based herbal syrup

Jessa Mae M. Laude[1^], Myra Ruth D. Picart[1^], Albebson L. Lim[1], Jortan O. Tun[1], Cydee Marie V. Ramones[1], Klidel Fae B. Rellin[2], Meljune O. Chicote[1], Eliza L. Belen[1], Ranjala Ratnayake[3], James H. Matthews[3], Hendrik Luesch[3], Lilibeth A. Salvador-Reyes[1], Gisela P. Concepcion*[1]

[1]The Marine Science Institute, University of the Philippines, Diliman, Quezon City 1101, Philippines
[2]Institute of Chemistry, University of the Philippines, Diliman, Quezon City 1101, Philippines
[3]Department of Medicinal Chemistry, University of Florida, Gainesville, Florida, U.S.A.

^contributed equally to the study

ABSTRACT

There is significant interest to use *Moringa oleifera* or "malunggay" as a source of anticancer and cancer chemopreventive agents to develop pharmaceutical drugs and herbal preparations. In this study, we isolated niazirin, niazinin, niazimicin, niaziminin and other glucosinolates, i.e., nitrile and O-thiocarbamate glycosides, from the ethanolic extract of *M. oleifera* seeds. These compounds were tested for antiproliferative activity in the MTT assay in human cancer cell lines, apoptotic activity in the annexin V/propidium iodide (PI) assay, antimigration activity in the matrigel wound healing assay, antiangiogenesis activity in the *in ovo* chorioallantoic membrane (CAM) assay, and activation of antioxidant response elements (ARE) in the ARE-luciferase reporter assay. The following activities were observed in the following compounds from seeds: antimigration and antiangionesis in niazirin; antimigration in niazinin; apoptosis, antimigration and antiangionesis in niazimicin; and antiproliferation and apoptosis in niaziminin. Several seed and leaf fractions activated ARE. We prepared a syrup formulation from an ethanolic leaf extract found to contain flavonoids, lipids and derivatives and a tetrapyrrole, which activated ARE and selectively inhibited SKOV-3 ovarian cancer cell line proliferation and showed no inhibition of the MDCK normal cell line.

*Corresponding author
Email Address: gpconcepcion@up.edu.ph
Date received: October 06, 2022
Date revised: December 13, 2022
Date accepted: December 20, 2022

KEYWORDS

Moringa oleifera, glucosinolates from seeds, syrup formulation of leaf extract with flavonoids, anticancer and cancer chemopreventive properties

INTRODUCTION

Carcinogenesis is a series of changes that accumulates in a normal cell and transforms it into a cell with uncontrolled proliferation (Loeb et al. 2008). Some carcinogens generate reactive oxygen species (ROS) that damage the DNA and promote procarcinogenic signaling (Waris and Ahsan 2006). This damage to the DNA could lead to mutations that confer tumor-sustaining abilities (e.g., sustained growth signaling, insensitivity to antigrowth signals, evasion of apoptosis, sustained angiogenesis, metastasis, and limitless reproductive potential to the cell) (Hanahan and Weinberg 2011).

Limiting the damage caused by ROS holds promise for cancer prevention and therapy (Wang et al. 2019). This can be achieved by antioxidants that scavenge ROS (Kotecha et al. 2016) or by antioxidant response elements (ARE), which enhance the production of detoxification enzymes and cytoprotective proteins.

The antioxidant-rich *Moringa oleifera* (Filipino name *malunggay*) is used in traditional Ayurvedic practice for cancer treatment and prevention (Meireles et al. 2020). *Moringa*'s chemoprotective potential has been attributed to glucosinolates and isothiocyanates (Fahey et al. 2018). These compound groups increase the activity of phase I and phase II liver enzymes, enzymes that metabolize xenobiotics resulting in their excretion from the body (Langner and Rzeski 2012). Phase II enzymes also engage the Keap-Nrf2 complex, which regulates the ARE signaling pathway (Michael and Doherty 2005; Tan and Spivack 2009). *M. oleifera* produces high yields of cancer preventive phytochemicals, from which stable and sustainable products can be prepared for consumption (Fahey et al. 2019).

In this study, we isolated compounds from the seeds and leaves of *Moringa oleifera* with anticancer and cancer chemopreventive properties using a bioassay-guided purification scheme. We report results from cancer cell line and normal cell line antiproliferative, apoptosis, antimigration, antiangiogenesis, and antioxidant assays. We prepared an oral herbal syrup formulation using a high-yield chromatographic fraction of the *Moringa* leaf extract with antioxidant and selective antiproliferative properties.

MATERIALS AND METHODS

General experimental section

Solvents were analytical grade (A.R., J.T. Baker), silica gel was 70-230 mesh (LiChroprep®, Sigma-Aldrich), analytical and preparative HPLC C18 columns were Phenomenex/Luna, and the HPLC with UV-VIS PDA unit was Shimadzu. All cell culture products were from Invitrogen unless otherwise specified. Propylene glycol and sorbitol were purchased from Sigma-Aldrich. Sucrose and sodium benzoate from Ajax Finechem.

All cell lines used in this study were acquired from American Tissue Culture Collection (ATCC), except for HK-2, a kind gift from Dr. Reynaldo Garcia of the National Institute of Molecular Biology and Biotechnology, University of the Philippines Diliman, and the MDA-MB-231 ARE-luc reporter cell line provided by Dr. Donna Zhang, University of Arizona. Cells were maintained in an incubator at 37 °C with 5% CO_2. All cell culture products were from Invitrogen unless otherwise specified. Cells were fed by changing the media every 2-3 days and subcultured (or used for assays) when they reached 70 to 90% confluency. Subculture was done by removing the spent media, washing with prewarmed 1x PBS three times, and detaching the cells from the flask with 0.25% trypsin-EDTA. The trypsin-EDTA was inactivated with fresh media before seeding them into new flasks (or multi-well plates for assays).

NMR spectra were obtained using a Varian spectrometer (500 MHz) at the Institute of Chemistry, U.P. Diliman or a Varian spectrometer (600 MHz) at the University of Utah. $CDCl_3$, CD_3OD, and $(CD_3)_2SO$ as solvents for 1D and 2D spectra. Positive- and negative-mode electrospray ionization-mass spectroscopy (ESI-MS) was performed using a Shimadzu LCMS-8040 (Shimadzu, Japan) at the Marine Science Institute, U.P. Diliman, and Waters UPLC-Xevo® G2-XS Quadrupole Time-of-Flight Mass Spectrometer (Waters, Milford MA, USA) at the Mass Spectrometry Facility, Institute of Chemistry, U.P. Diliman.

Graphs, calculations, and statistical analysis were done in GraphPad Prism version 7.0 (GraphPad Software, San Diego, CA, USA) and Microsoft Excel (Microsoft Corporation, Albuquerque, NM, USA).

Sample collection, preparation and labeling

Plant materials (leaves and fruits) were obtained from a *Moringa oleifera* tree in a secluded site in Angat, Bulacan. The materials were washed with tap water and segregated by anatomical parts (leaflets were removed from stems and seeds from fruits) before air-drying at room temperature or oven-drying at 50°C. The drying process commenced within 2 h of collection. The dried samples were pulverized using a blender and stored at room temperature. For the upscale extraction, plant materials were collected from the Green Earth Heritage Foundation, Inc. (GEHFI) in Santa Maria, Bulacan, which has an extensive Moringa organic farm.

Samples were labeled systematically to indicate the plant material (S = seeds, L = intact mature leaves), drying method (A = air-drying, O = oven-drying), and extraction solvent (E = ethanol). This is followed by the solvent/s (if any) used to partition the ethanolic extract (H = hexane, C = chloroform, E = ethyl acetate), and the fraction number (OCF1, OCF2, etc. for open column fractions; F1, F2, etc. for HPLC fractions). U indicates upscale extraction, e.g., ULOE extract. Dashes indicate purification steps. For example, air-dried seeds soaked in ethanol, partitioned in chloroform, eluted as the fourth fraction in open column chromatography, and eluted as the third fraction in HPLC would have the code SAE-C-OCF4-F3 (**SI Fig. 1**).

Extraction, isolation and purification

The dried plant material was soaked in ethanol (1 g:10 mL) thrice overnight; soakings were filtered, and the supernatant was dried *in vacuo* (Buchi rotary evaporator) at 36°C. To identify priorities for purification, the dried extracts were weighed to obtain yields, and screened for biological activity.

Ethanol extract from air-dried seeds (SAE)

The SAE crude extract was concentrated *in vacuo* (Buchi rotary evaporator) at 36°C to give ~5 g of concentrate. A portion (1 g) was fractionated by the modified Kupchan partitioning method (Van Wagenen et al. 1993) into the n-hexane, chloroform, ethyl acetate, and aqueous soluble fractions.

The n-hexane extract (~300 mg) was fractionated using normal phase open column chromatography (silica gel, 40-63 µm, 1.1 x 8.8 cm) using hexane and increasing proportions of ethyl acetate at 10% increments to afford 13 fractions.

The chloroform partition (~207 mg) was chromatographed on an open silica gel column (70-230 mesh; 1.1 x 8.8 cm) and eluted with increasing proportions of acetone in dichloromethane at 10% increments to give 13 fractions. Fractions were dried, quantified, and tested for antiproliferative activity, and HPLC was performed on the most active fraction (**SI Fig. 2**).

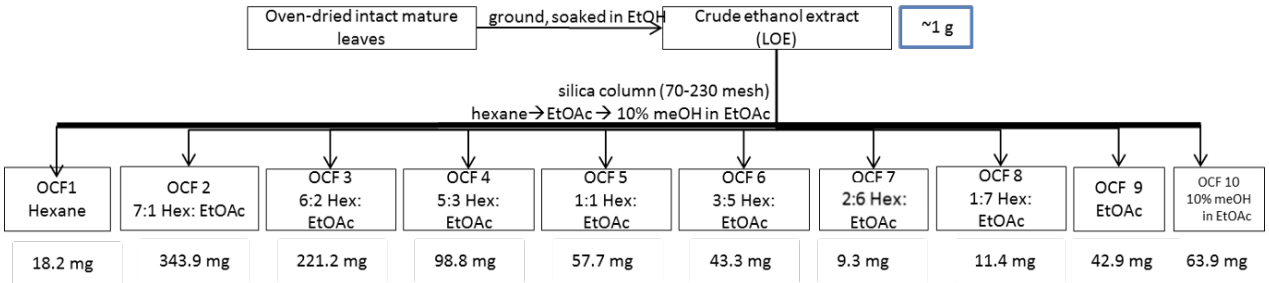

Figure 1: Extraction and open column chromatography of *Moringa* leaves (ULOE-OCF: upscale extraction of leaves, oven-dried, ethanol, open column fraction).

Ethanol extract from oven-dried intact mature leaves (ULOE)

The intact mature leaves from GEHFI (100 kg) were oven-dried instead of air-dried due to the large quantity (U=Upscale). Leaves were soaked in ethanol, filtered, and dried In vacuo. The ULOE crude ethanol extract was chromatographed in an open silica gel column and eluted with increasing proportions of ethyl acetate in n-hexane (OCF1–8), followed by pure ethyl acetate (OCF9) and 10% methanol in ethyl acetate (OCF10). (**Fig. 1).**

Chemical profiling and structure identification

Purification of compounds from seeds by high performance liquid chromatography (HPLC)

Compound separation was done using a semipreparative C_{18} column (Phenomenex Luna, 5 µm particle size, 300 Å pore size, 10 mm X 250 mm) at 3 mL/min flow rate using a CH_3CN in water gradient (30% CH_3CN for 10 min, 30–100% CH_3CN in 10 min, 100% CH_3CN for 5 min). Elution was monitored at 220 nm, 254 nm, and 360 nm using a photodiode array detector.

These are the corresponding retention times of the SAE-C-OCF4 fractions: SAE-C-OCF4-F1, t_R=9.0 min; SAE-C-OCF4-F2, t_R=10.0 min; SAE-C-OCF4-F3, t_R=12.0 min; SAE-C-OCF4-F4, t_R=17.0 min; SAE-C-OCF4-F5, t_R=21.0 min; and SAE-C-OCF4-F6, t_R=22.0 min (**SI Fig. 3**).

Unidentified compound (SAE-C-OCF4-F1): UV (ACN:H_2O + 0.1% TFA) λ_{max}220, 254; ^{1}H NMR and ^{13}C NMR data (**SI Fig. 11)**.

Niazirin (SAE-C-OCF4-F2): UV (ACN:H_2O + 0.1% TFA) λ_{max}254; LC-ESIMS m/z 297.17 $[M+NH_4]^+$ (niazirin, MW = 279.29); ^{1}H NMR and ^{13}C NMR data, see **SI Fig. 8**.

Unidentified compound (SAE-C-OCF4-F3): UV (ACN:H_2O + 0.1% TFA) λ_{max}254 **(SI Fig. 10)**.

Niazinin (SAE-C-OCF4-F4): UV (ACN:H_2O + 0.1% TFA) λ_{max}254; LC-ESIMS m/z 344.060 $[M+H]^+$ (niazinin, MW = 343.4); ^{1}H NMR and ^{13}C NMR data, see **SI Fig. 6**.

Niazimicin (SAE-C-OCF4-F5): UV (ACN:H_2O + 0.1% TFA) λ_{max}254; LC-ESIMS m/z 358.07 $[M+H]^+$, m/z 380.07 $[M+Na]^+$, and m/z 356.17 $[M-H]^-$ (niazimicin, MW = 357.4); ^{1}H NMR and ^{13}C NMR data, see **SI Fig. 5**.

Niaziminin (SAE-C-OCF4-F6): white solid; UV (ACN:H_2O + 0.1% TFA) λ_{max}195 nm, 222 nm, and 240-280 nm (broad); ^{1}H NMR and ^{13}C NMR data, see **SI Fig. 12**.

Identification of compounds from leaf extract by mass spectrometry (MS) and molecular networking

Compounds in the ULOE-OCF10 extract were identified based on mass spectrometry (MS) data which was matched to known compounds in the cloud-based bioinformatics platform Global Natural Products Social Molecular Networking (Wang et al. 2016) adapting a previously reported protocol (Molino et al. 2021). Library matching was performed using the following parameters: precursor ion mass tolerance of 0.45 Da, fragment ion mass tolerance of 0.50 Da, a minimum cosine (similarity) score of 0.70, and minimum matched peaks of 6. To create molecular networks that aided in the annotation of the compounds, the same platform was used following these parameters: minimum similarity (cosine) of 0.70 calculated from the fragmentation pattern of two precursor ions, six matched peaks, and a maximum number (top K) of 7 neighbors. Values for these analyses were optimized according to the type of instrument and data acquired for this study. Network visualization was customized using Cytoscape 3.7.1 (Shannon et al. 2003).

Quercetin: HRESIMS m/z 303.0518 $[M+H]^+$ (monoisotopic mass, Da = 302.0427).

Quercetin-3-O-hexoside: HRESIMS m/z 465.1011 $[M+H]^+$, (monoisotopic mass, Da = 464.0955).

Isoquercitrin: HRESIMS m/z 463.0875 $[M-H]^-$, (monoisotopic mass, Da = 464.4).

Kaempferol: HRESIMS m/z 287.0584 $[M+H]^+$ (monoisotopic mass, Da = 286.0477).

Kaempferol-3-O-glucoside: HRESIMS m/z 447.0986 $[M-H]^-$ (monoisotopic mass, Da = 447.0927).

13-Docosenamide: HRESIMS m/z 338.3420 $[M+H]^+$ (monoisotopic mass, Da = 337.3345).

GalCer(d18:2/20:1): HRESIMS m/z 752.5034 $[M+H]^+$ (monoisotopic mass, Da = 751.5962).

Pheophorbide A: HRESIMS m/z 593.2755 $[M+H]^+$ (monoisotopic mass, Da = 592.2686).

Vitexin: HRESIMS m/z 431.0971 $[M-H]^-$ (monoisotopic mass, Da = 432.1056).

Mammalian cell culture and MTT antiproliferation assay

The cancer cell lines used were human breast adenocarcinoma (MCF-7), human ovary adenocarcinoma (SKOV-3), human colorectal carcinoma (HCT 116) and human non-small cell lung carcinoma (A549). To test for selective antiproliferative activity in cancer cells, extracts/ and compounds were also tested for nephrotoxicity and hepatotoxicity. For nephrotoxicity, kidney cell lines that originated from normal tissues were used, such as normal dog kidney (MDCK), normal human proximal tubular kidney (HK-2), and African green monkey kidney (Vero) cell lines. For hepatotoxicity, human hepatocellular carcinoma

(HepG2), a common *in vitro* model for human liver cells, was used. Culture conditions can be found in **SI Table 1.**

The assay was done based on Mosmann (1983) with slight modifications. Briefly, the cells were seeded into a 96-well plate and incubated for 24 h at 37ºC with 5% CO_2. The seeding densities for each cell line were optimized based on their growth curves. Samples were suspended in DMSO and screened at two concentrations (50 µg/ml and 5 µg/ml). Doxorubicin (1 µM or 0.54 µg/mL and 0.1 µM or 0.054 µg/mL) and DMSO (1% v/v) were used as positive and negative controls, respectively. After 72 h, media was discarded, and 15 µL of 5 mg/ml MTT (Molecular Probes) in 1X PBS was added to each well. The plates were incubated for 3 h at 37ºC, 5% CO_2, and then 100 µl DMSO was added to each well to solubilize the formazan products. Absorbance was measured at 570 nm using a microplate reader (Biotek Synergy™ HT, Biotek, United States). Each treatment was performed in triplicate with at least two independent experiments.

The % inhibition of each extract was calculated using the following formula:

$$\%\ inhibition = \left[1 - \left[\frac{absorbance_{extract} - absorbance_{blank}}{absorbance_{solvent\ control} - absorbance_{blank}}\right]\right] \times 100$$

Extracts that caused >60% inhibition were considered significantly active, while those in the 40-60% inhibition range were considered slightly active. Assay was done in quadruplicate with three independent trials.

Annexin V/propidium iodide (PI) apoptosis assay

This assay was done based on the Annexin V-FITC Apoptosis Detection Kit (BD Pharmingen), with slight modifications. MCF-7 cells were grown in 6-well plates at 6.7 x 10^5 cells/well. After 24 h, cells were treated with fractions or compounds (5 and 50 µg/mL), 100 µM paclitaxel (positive control), or 0.1% v/v DMSO (negative control) for 66 h at 37°C. Subsequently, cells were washed once with cold 1X PBS, spun at 300*g,* and resuspended in 600 µL of 1X binding buffer (140 mM NaCl, 4 mM KCl, 0.75 mM $MgCl_2$ and 10 mM HEPES, 1.75 mM $CaCl_2$ (Trahtemberg et al. 2007)) yielding ~1 x 10^6 cells/mL. Then, 100 µL of the cell suspensions were stained with 5 µL Annexin V and 5 µL propidium iodide. After 15 min incubation at room temperature in the dark, 400 µL of 1X binding buffer was added. Finally, cells were analyzed using a flow cytometer (BD FACSCalibur, BD Biosciences, India) at FL-1 (λ_{em} ~530 nm) and FL-2 (λ_{em} ~585 nm) channels. Density plots and percentage of FITC-Annexin V- and PI- stained cells were obtained using BD CellQuest software**.** The assay was performed in one replicate in a single independent trial.

Matrigel wound healing antimigration assay

The matrigel wound healing assay was performed as described by Liang et al. (2007). Cells were seeded onto a layer of matrigel (50 µg/mL) in the wells of a 96-well plate, and allowed to grow to 100% confluence. A cross-shaped scratch was then made in each well using a 10-µL pipet tip. The spent media was removed and the cells were washed to remove the remaining debris. Fresh media was added to the cells, treated with the samples (5 µg/mL and 50 µg/mL, 0.1% DMSO (vehicle control) or LY294002 (PI3K inhibitor used as positive control; 3.8 µg/mL and 38.4 µg/mL) and incubated for 48 h at 37ºC with 5% CO_2.

Photographs of the cells were taken at 0 h (before treatment) and after 48 h of treatment. The distances the cells migrated were then measured using the software ImageJ 1.48 (Wayne Rasband, National Institutes of Health, USA), and the migration index was calculated as follows:

$$\%\ migration = \frac{distance\ migrated\ by\ treated\ cells}{distance\ migrated\ by\ cells\ treated\ with\ solvent\ control}$$

$$migration\ index = \frac{\%\ migration}{\%\ cell\ viability}$$

A low migration index indicates antimigratory activity. The assay was done in triplicate with three independent trials.

***In ovo* chorioallantoic membrane (CAM) antiangiogenesis assay**

This assay was adapted from Raga et al. (2011). Fertile Longhorn chicken eggs were obtained from a commercial supplier from Silang, Cavite. Day 0 eggs (n = 3) were incubated at 37°C. On day 7, a 4-cm^2 window was made and sealed with a sterile laboratory film. On the 8th day of incubation, 5 µL of the samples were added to the sterile 5 x 5 mm filter discs to obtain the final concentrations of 25 µg (high dose) and 2.5 µg (low dose). At the end of the 72-h incubation, the CAMs were cut and observed at 400x magnification under an inverted microscope (Olympus IX51, Olympus, Japan).

The scoring of blood vessel formation was adapted from Burdick et al. (2003). Branching and blood vessels were quantified using the software ImageJ 1.40 (Wayne Rasband, National Institutes of Health, USA) with the Analyze Skeleton plugin created by the U.S. National Institutes of Health. Significant differences between the values were analyzed using the two-tailed T-test for paired samples. A $p<0.05$ was considered significant. The assay was performed in triplicate with one independent trial.

Antioxidant response elements (ARE)-luciferase reporter assay

The ARE-luciferase reporter assay (Matthews et al. 2018 and Ratnayake et al. 2013) was performed using a stably transfected breast adenocarcinoma, MDA-MB-231 ARE-luc reporter cell line for ARE inhibition and the prostate cancer cell line LNCaP for ARE activation. ARE luciferase reporter plasmid (50 ng/well) and CMV-GFP (10 ng/well) plasmid for monitoring transfection efficiency were co-transfected into LNCaP cells using FugeneHD (Roche). MDA-MB-231 ARE-luc cells (1 x 10^4 cells/well) and transfected LNCaP cells (2 x 10^4 cells/well) were seeded in 96-well plates and incubated at 37 □C with 5% CO_2 for 24 h. The cells were treated with the samples (1 µg/mL, 10 µg/mL, and 100 µg/mL), with 10 µM sulforaphane or 125 nM brusatol (positive controls for ARE activation and inhibition, respectively) and DMSO (negative control). Luciferase activity was measured 24 h after sample treatment using BriteLite detection reagent (PerkinElmer) following manufacturer's protocol; luminescence was read with an Envision (PerkinElmer) plate reader. Cell viability assay was carried out in parallel for both experiments and assessed using MTT according to the manufacturer's protocol (Promega). ARE activation and inhibition were measured as a function of the luminescence produced by the cells and normalized to the negative control (DMSO). All assays were carried out in triplicate experiments.

Syrup formulation of ULOE-OCF10

Herbal syrup formulation of ULOE-OCF10 was prepared as presented in **Table 1**, adapted from Niazi (2019). The simple syrup was prepared from sucrose dissolved in purified water and heated (30-40°C) with continuous stirring. The excipients were

Table 1: Formulation for ULOE-OCF10[a]

Components	Function	Formulations			
		1	2	3	4
Simple Syrup[b] (mL)	Sweetener	5	5	5	5
Sorbitol (g)	Vehicle	23	40	23	500
Propylene glycol (mL)	Solvent	0.5	0.5	0.5	0.5
Sodium benzoate (mg)	Preservative	107	111	14	14
Purified water (mL)	Vehicle	to 10 mL	to 10 mL	to 10 mL	to 10 mL

[a]The concentration of the active extract (ULOE-OCF10) was 100 µg/mL.
[b]Simple syrup was prepared by dissolving 85 g sucrose (for formulations 1 to 3) or 66.7 g (for formulation 4) in 100 mL distilled water.

combined with the simple syrup, ULOE-OCF10 extract (100 µg/mL), and purified water. Dissolution was ensured by stirring at room temperature. The herbal syrup was stored in amber bottles at room temperature (25°C) or refrigerated at 4°C and evaluated for physical stability (color, odor, taste, pH, and precipitation) for 28 days.

RESULTS AND DISCUSSION

1. Chemical characterization of bioactive compounds from *M. oleifera* seeds and leaves

1.1. *Ethanol extract from air-dried seeds (SAE)*

The chloroform partition from the ethanolic air-dried seed extract (SAE-C) afforded 13 silica open column fractions (SAE-C-OCFs), with fractions 1–5 showing significant activity against several cancer cell lines. SAE-C-OCF4 (open column fraction 4, 30% acetone in DCM) showed antiproliferative activity against all cancer cell lines tested (MCF-7, A549, HCT 116 and SKOV-3) with minimal activity (<60-40% inhibition) against normal kidney cells (Vero). SAE-C-OCF4 purification afforded six fractions. NMR and MS analysis were done to determine the structures of the purified compounds (**Fig. 2**).

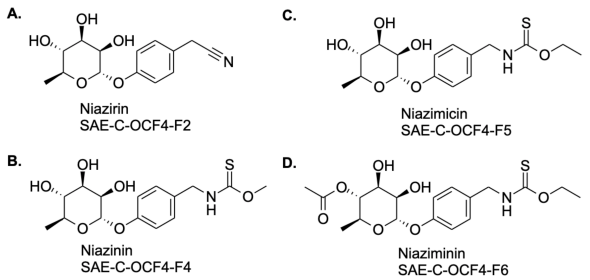

Figure 2: Compounds from ethanolic extracts of *M. oleifera* air-dried seeds

1.1.1. *SAE-C-OCF4-F2*

We identified SAE-C-OCF4-F2 as niazirin (**Fig. 2A**). ^{1}H NMR data showed chemical shifts such as aromatic (δ_H 7.29 & 7.08), anomeric (δ_H 5.43), methyl attached to a sugar moiety (δ_H 1.21), and protons attached to a sugar moiety (δ_H 3.0-4.0), suggesting that this compound is a glucosinolate derivative. Protons of the methoxy (δ_H 3.95) and ethoxy (δ_H 4.47) groups were not observed in SAE-C-OCF4-F2, instead the benzylic proton chemical shift was seen at δ_H 3.83. The ^{13}C signal at δ_C 119.8 is indicative of a nitrile group. COSY established the connectivity of the protons. These observations confirmed SAE-C-OCF4-F2 as niazirin. ^{1}H and ^{13}C NMR chemical shift assignments of SAE-C-OCF4-F2 are in agreement with the reported data for niazirin (Maurya et al. 2011).

1.1.2. *SAE-C-OCF4-F4*

SAE-C-OCF4-F4 was identified as niazinin (**Fig. 2B**). The anomeric proton (δ_H 5.41) and a methyl doublet (δ_H 1.22) supported the assignment of the sugar as rhamnose. Signals from δ_H 3.45 - 3.99 (with 1H integration each) confirmed the sugar moiety. The two-proton mutually coupled doublets (ca. δ_H 7.25 and 7.00) point to a p-substituted benzene ring in the molecule. A signal at δ_H 4.64 indicated the presence of benzylic methylene. A methyl singlet at δ_H 3.95 also indicates a methoxy group for niazinin. Positive-ion ESI-MS analysis revealed a neutral mass of 343 for SAE-C-OCF4-F4, further corroborating the compound's identity as niazinin (Huang et al. 2020).

1.1.3. *SAE-C-OCF4-F5*

SAE-C-OCF4-F5 was identified as niazimicin (**Fig. 2C**), a structural analog of niazinin. All proton signals found in SAE-C-OCF4-F4 were present in F5 except for the methoxy protons at δ_H 3.95. Instead, signals at δ_H 4.47 and δ_H 1.29, corresponding to the ethoxy moiety, were observed. Low-resolution mass spectrometry (ESI, positive and negative-ion mode detection) analysis of SAE-C-OCF4-F5 revealed an m/z of 357, with a mass difference of 14 Da with niazinin, confirming the identity of SAE-C-OCF4-F5 as niazimicin (Atolani et al. 2020).

1.1.4. *SAE-C-OCF4-F6*

SAE-C-OCF4-F6 was identified as niaziminin (**Fig. 2D**). ^{1}H NMR data of this compound showed striking similarity to niazinin and niazimicin, with signals corresponding to aromatic (δ_H 7.00 –7.50), anomeric (δ_H 5.44), benzylic (δ_H 4.63 and δ_H 4.70), methoxy (δ_H 1.20–1.22, t) and sugar moiety (δ_H 3.00 – 4.00) protons (**SI Fig. 12**). This suggests that these compounds belong to the same structural class. The presence of a singlet at δ_H 2.03 indicates an acetoxy substituent. Based on the literature, this fraction matches the NMR description of niaziminin (Faizi et al. 1992).

Niazinin and niazirin were previously reported as hypotensive agents and one of the first naturally occurring thiocarbamates (Faizi et al. 1992; Saleem 1995), while niazimicin was shown to be a potent antitumor promoter in a two-stage carcinogenesis mouse skin model (Guevara et al. 1999). Niaziminin is the acetyl derivative of niazimicin (Faizi et al. 1992). Murakami et al. (1998) reported that niaziminin showed considerable inhibition against Epstein-Barr Virus (EBV) activation. Structure-activity studies indicated that the acetoxy group at the 4'-position of niaziminin is indispensable for this inhibition.

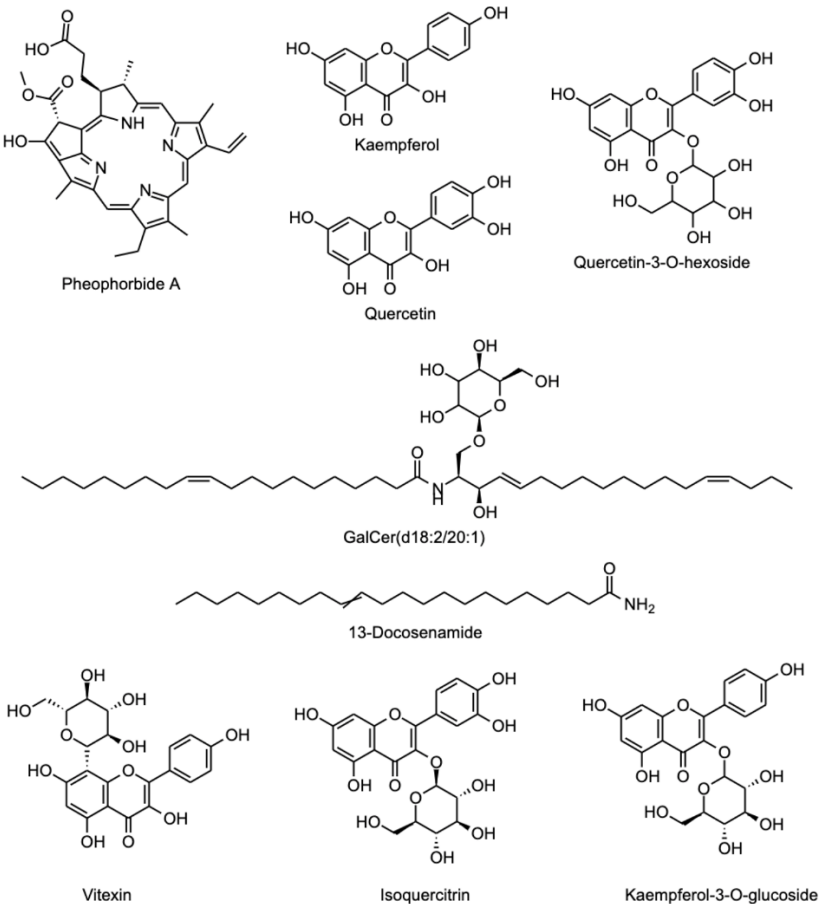

Figure 3: Compounds from the ethanolic extracts of *M. oleifera* oven-dried intact mature leaves. Mass spectra can be found in the Supporting Information.

1.1.5. *Unidentified compounds*

Two pure fractions SAE-C-OCF4-F1 and SAE-C-OCF4-F3 showed characteristic signals for glucosinolates in their 1H NMR spectra. However, insufficient yield and poor ionization in MS prevented the identification of these compounds.

1.2. *Upscale ethanol extraction from oven-dried intact mature leaves (ULOE)*

To prepare a cancer chemopreventive *Moringa* leaf extract into a herbal syrup formulation and to scale up its production, leaves were chosen over seeds as the source of material suitable based on its sustainability, i.e. regular harvest leaves from trees as opposed to harvest of fruits and seeds required for replanting. The ULOE-OCF10 fraction used in the syrup preparation was chemically profiled by HPLC and UV-VIS (**SI Fig. 4B**) and not further purified to maximize incorporation of the identified phytochemicals in the mixture. **Fig. 3** shows the constituents identified.

High resolution ESI-MS under positive and negative ionization modes (**SI Fig. 14 and 15**) was used to determine the compounds in ULOE-OCF10, the most promising fraction based on the activities detailed in the succeeding discussion. GNPS annotation identified the following compounds from the networks generated from the positive-mode tandem MS: quercetin-3-*O*-hexoside (m/z), quercetin (m/z), kaempferol (m/z), 13-docosenamide, d18:2/20:1-galactosylceramide and pheophorbide A (**Fig. 3**). Networks generated from the negative-mode tandem MS were annotated as the following: vitexin and kaempferol-3-*O*-glucoside. The negative mode data also presents the negative ion adduct $[M-H]^-$ of quercetin-3-*O*-hexoside.

Quercetin inhibits cancer cell proliferation (Hertog et al. 1993) by causing apoptosis (Lee et al. 2006). Sugar derivatives of quercetin also demonstrate antioxidant and chemopreventive properties (di Camillo Orfali et al. 2016). Derivatives of galactosylceramides demonstrate activity against breast cancer (Kikuchi et al. 2001), melanoma (Nakagawa et al. 2001), and inflammation (de los Reyes 2016). Vitexin mitigates damage from ROS by donating electrons to reduce radicals (Babaei et al. 2020). Kaempferol and its derivatives exert strong antioxidant properties and are known to affect proliferation and apoptosis of cancer cells (Kluska et al. 2021). Pheophorbide A, a tetrapyrrole derived from chlorophyll, is a photosynthesizer that can induce antiproliferative effects in several human cancer cell lines (Saide et al. 2020).

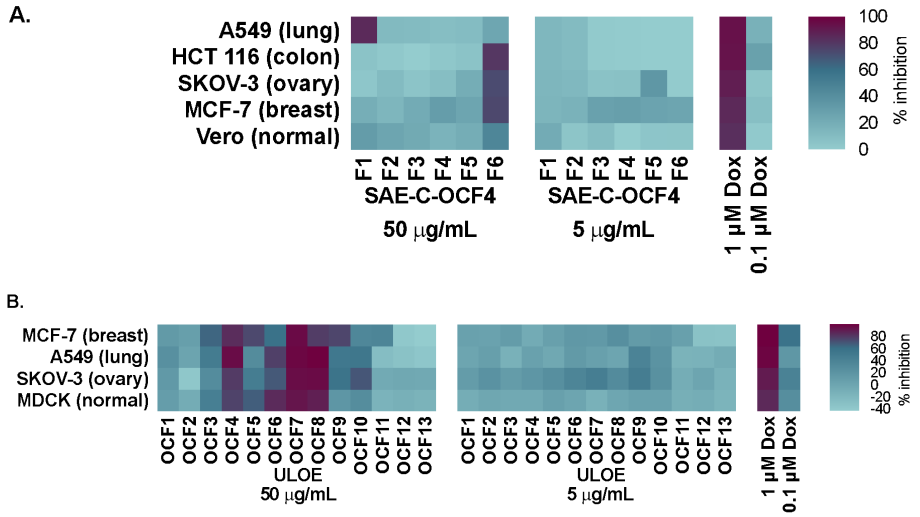

Figure 4: Antiproliferative activity against cancer cells and normal kidney cells of *Moringa* fractions: (**A**) HPLC fractions from the open column fraction 4 of the chloroform partition of ethanolic seed extract (SAE-C-OCF4-Fs) and (**B**) upscale open column fractions from the ethanolic oven dried leaf extract (ULOE). Cells used in the assay were less than passage 20. Data presented as mean of three independent trials.

Table 2: Selectivity indices of some of the ULOE-OCFs

ULOE-OCFs	IC_{50} (µg/mL)[a]				Selectivity Index[b]		
	SKOV-3	HK-2	HepG2	MDCK	HK-2 /SKOV-3	HepG2 /SKOV-3	MDCK /SKOV-3
OCF 7	32.46	54.88	38.13	nt[c]	1.69	1.17	nt[c]
OCF 8	37.34[a]	36.54	34.41	nt[c]	0.98	0.92	nt[c]
OCF 9	48.42	41.22	34.69	72.38	0.85	0.72	1.49
OCF10	31.93	nt[c]	nt[c]	72.62	nt[c]	nt[c]	**2.27**

[a]IC_{50} against A549 lung cancer cells. IC_{50} is the concentration that inhibits the growth of 50% of the cells. Data represents mean of four replicates.
[b]Selectivity Index was calculated by dividing the IC_{50} on normal cell lines over the IC_{50} on cancer cell lines. Selectivity Index > 1 means that the extract preferentially kills the cancer cells over the normal cells.
[c]not tested

2. Bioactivity assessment

2.1. *Antiproliferative activity of compounds F1-6 from seeds and extract ULOE-OCF10 from leaves in mammalian cell lines*

Of the six compounds isolated from seeds (SAE-C-OCF4-F1 to F6), two displayed antiproliferative activity to cancer cells (**Fig. 4A**). SAE-C-OCF4-F1 inhibits A549 non-small cell lung cancer cell proliferation (84.8%) but not the proliferation of other cancer cells at 50 µg/mL. Moreover, SAE-C-OCF4-F1 is noncytotoxic to Vero normal kidney cells (31.6%). This This selective activity of SAE-C-OCF4-F1 against lung cancer cells makes it a promising antitumor agent. SAE-C-OCF4-F6, putatively identified as niaziminin, is the most active, showing activity against the following cancer cell lines: HCT 116 colon (80.4%), SKOV-3 ovarian (73.1%), and MCF-7 breast (74.3%) cancer cells, not to A549 lung (24.8%), and only slightly active against Vero normal kidney cells (45.9%) at 50 µg/mL. This supports the data of Murakami et al. (1998) showing antitumor promoting activity of niaziminin. The other compounds niazirin (F2), niazinin (F4), niazimicin (F5), and F3 did not inhibit cancer cell and normal kidney cell proliferation.

The fractions from the leaves, ULOE-OCF4, ULOE-OCF7, and ULOE-OCF8, exhibited antiproliferative activity against all cell lines, including the normal MDCK cell line (**Fig. 4B**). ULOE-OCF5 inhibited MCF-7 and MDCK cell proliferation while ULOE-OCF6 showed antiproliferative activity in A549, SKOV-3, and MDCK cells. ULOE-OCF9 and ULOE-OCF10 selectivity inhibited the proliferation of breast (74.8%) and ovarian cancer cells (69.1%), respectively; no inhibition was observed against MDCK cells (16.8% and 27.5%, respectively). The dose-response curves and IC50s of ULOE-OCF10 in SKOV-3 ovarian cancer cells and MDCK normal kidney cells indicated selective antiproliferative activity against SKOV-3 (**SI Fig. 16).** ULOE-OCF10 showed a selectivity index of 2.27 (**Table 2**), and hence was selected as the active ingredient for the syrup formulation.

2.2. *Apoptotic activity*

Annexin V is a Ca^{2+}-dependent phospholipid-binding protein that has a high affinity for the phospholipid phosphatidylserine (PS). The dye propidium iodide (PI) is useful for quantifying early apoptotic cells. During the early stage of apoptosis, cells lose their membrane asymmetry, and PS is translocated from the inner leaflet of the plasma membrane to the outer leaflet, exposing PS to the environment. When used in tandem with PI, we can distinguish apoptotic from dead or necrotic cells. Cells that stain positive for Annexin V and negative for PI are undergoing apoptosis. Cells that stain positive for both Annexin V and PI are either in the end stage of apoptosis, are undergoing necrosis, or are already dead. Cells that stain negative for both Annexin V and PI are alive and not undergoing measurable apoptosis.

Fractions were prioritized based on their activity in the MTT assay and tested for apoptotic activity using the FITC-Annexin V/PI flow cytometry assay. Briefly, MCF-7 human breast adenocarcinoma cells were treated with the fractions, 0.1% DMSO (vehicle or negative control) and paclitaxel (positive control). The cells were then incubated with the sample or control (60 h for control, LOE fractions, SAE-C-OCF4, and SAE-C-OCF4-F6; 30 h for SAE-C-OCF4-F4 and SAE-E-OCF4-F5) before staining for flow cytometry.

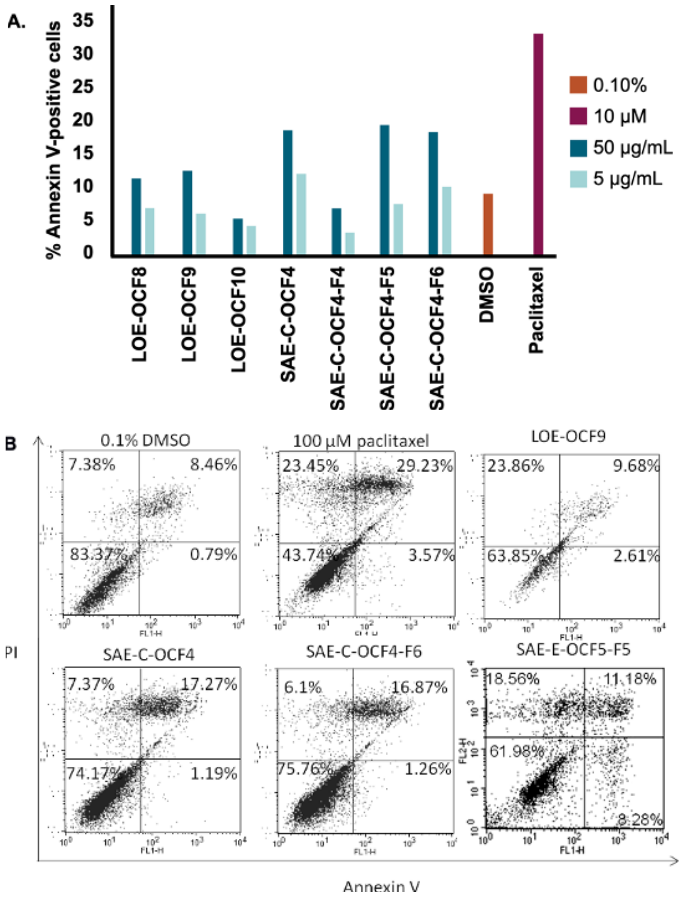

Figure 5: Apoptotic activity of column fractions from *Moringa* ethanolic seed and leaf extracts. (A) % Annexin V positive MCF-7 cells treated with *Moringa* compounds/fractions for 60 h, except for SAE-C-OCF4-F4 and SAE-E-OCF5-F5, for which sample incubation lasted 30 h. 0.1% DMSO and paclitaxel (5.86 µM) served as negative and positive controls, respectively. **(B)** Representative dot plots (bottom) of MCF-7 cells treated with sample at 50 µg/mL.

Fig. 5 shows the samples that were positive in Annexin V (both early and late apoptosis). SAE-C-OCF4, SAE-E-OCF4-F5, and SAE-C-OCF4-F6) were positive for Annexin V. SAE-C-OCF4-F6 (niaziminin) inhibited the proliferation of several cell lines and results from this assay suggest that the mode of cell death induced by this compound is via apoptosis. SAE-C-OCF4-F4 (niazinin) did not show apoptotic activity which is in agreement with its lack of activity in the MTT assay. SAE-E-OCF5-F5 (niazimicin) showed high apoptotic activity after 30 h of treatment. This stimulation of apoptosis is not enough to measurably counteract MCF-7 proliferation in the MTT assay; other hallmarks that confer malignancy to MCF-7 could still enable the cell population to grow (Comşa et al. 2015).

LOE-OCF10 showed no apoptotic activity. This could be due to the selective antiproliferative activity of LOE-OCF10 in SKOV3 ovarian cancer cells. LOE-OCF8 and OCF9 showed antiproliferative activity against MCF-7 (**Fig. 4B**) but showed low number of Annexin V positive cells. One possible explanation is that these fractions do not induce cell death through apoptosis. Another is that the cells may also have undergone cell death at an earlier time point. The time of assay may not capture the transient nature of apoptosis; this could be resolved by time course flow cytometry experiments or measure real-time cytotoxicity.

2.3. *Antimigration*

The compounds or fractions from seeds (SAE-C-OCF4 and SAE-C-OCF4-F1 to F6) and leaves (LOE-OCF1 to OCF10) were assayed for antimigration activity. After 48 h, untreated and vehicle-treated A549 non-small cell lung carcinoma cells showed no inhibition of migration or wound closure. LY294002-treated cells showed high and concentration-dependent inhibition of migration. The calculated migration indices are shown in **Fig. 6**, where migration index (M.I.) <1 indicates inhibition of migration of A549 cells.

LY294002 acts by inhibiting phosphoinositide-3-kinase (PI3K), a signaling protein involved in the expression of the matrix metalloproteinases (MMPs), which are key players in metastasis and invasion (Shen et al., 2014). LY294002 shows a dose-dependent inhibition of migration (% migration) of A549 cells, no cytotoxicity to A549 cells at both concentrations (high % viability), and thus a low M.I. From the upscale leaf extract ULOE, OCF fractions 1-10 showed dose-dependent inhibition of migration (% migration) in varying degrees relative to the solvent control; however this semi-quantitative measurement, i.e., distance of migration, does not measure the number of viable A549 cells remaining after 48 h. It is noted that ULOE-OCFs 4, 6, 7, and 8 are cytotoxic at 50 µg/mL based on the MTT assay (see also Fig. 4), M.I.s at this dose are low and the dose-dependence trend for M.I. is reversed, indicating that this cytotoxic concentration would not be suitable to achieve an

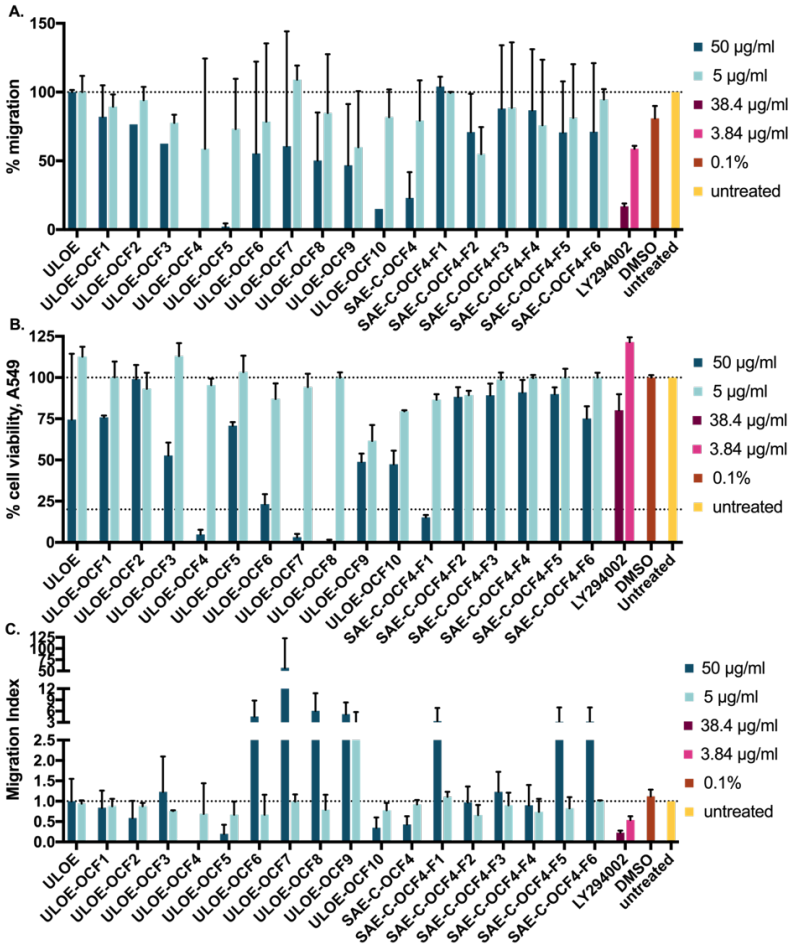

Figure 6: Antimigration activity of compounds/fractions from *Moringa* seeds or leaves. A549 lung cancer cells were treated with the sample for 48 h. (**A**) Percent migration and (**C**) migration index (M.I.) were calculated as described in Materials and Methods. (**B**) Percent viability of A549 cells was determined by the MTT assay (see Fig. 4). Migration indices <1 indicate inhibition of migration of A549 lung cancer cell. LY294002 and DMSO were used as positive and negative controls, respectively. Migration index represents mean ± SD (n=3).

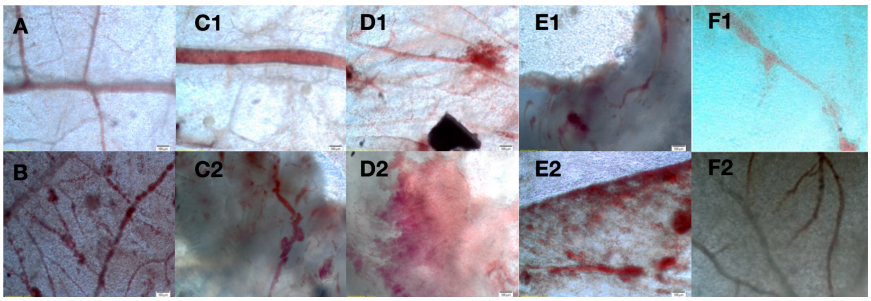

Figure 7: Chorioallantoic membranes of eggs that were (**A**) untreated, or (**B**) treated with DMSO, (**C1**) 25 µg endostatin, (**C2**) 2.5 µg endostatin, (**D1**) 25 µg SAE-C- OCF4-F6, (**D2**) 2.5 µg SAE-C- OCF4-F6, (**E1**) 25 µg SAE-H-OCF9-F7, (**E2**) 2.5 µg SAE-H-OCF9-F7, (**F1**) 25µg ULOE-OCF4 and (**F2**) 2.5µg ULOE-OCF4.

antimigration effect. On the other hand, ULOE-OCF5 and ULOE-OCF10 at 50 µg/mL showed low % migration and high % cell viability, and low M.I. values of 0.13 and 0.18, respectively. SAE-C-OCF4 from the seeds showed a smaller decrease in % migration at 50 µg/mL than at 5 µg/mL, indicating the presence of cytotoxic compounds, i.e., SAE-C-OCF4-F1 which was shown to be cytotoxic to A549 cells (see also **Fig. 4**). Compounds F2-6 showed modest to low reduction in % migration and are noncytotoxic to A549 cells at 5 µg/mL.

2.4. *Antiangiogenesis*

The *in ovo* chorioallantoic membrane (CAM) assay is widely used to assess the antiangiogenic properties of a compound. The CAM is an extraembryonic membrane that is rich in blood vessels where exchange of gases for the growing embryo happens. Further, the CAM contains extracellular matrix proteins which mimic the physiological cancer environment (Lokman, et al. 2012).

Tumor angiogenesis is a target for the suppression of metastasis. To characterize the antiangiogenic property of *Moringa* seeds and leaves, the chorioallantoic membrane (CAM) assay was

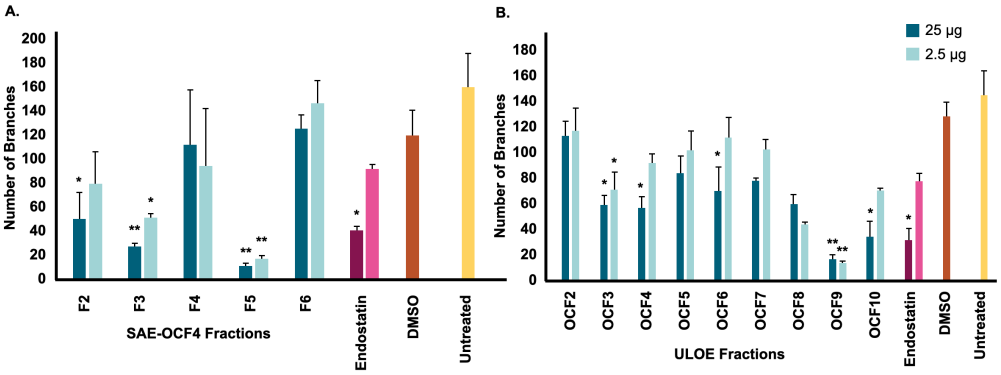

Figure 8: Antiangiogenic property of compounds from *Moringa* ethanolic seed extracts. Branching point analysis of chorioallantoic membranes (CAMs) of eggs that were treated with (**A**) compounds (SAE-C-OCF4-F2 to F6) from seeds and (**B**) fractions (LOE-OCF1 to OCF10) from leaves (bottom) for 72 h. At least three eggs were used per treatment. Bar represents mean ± SD (n=3). *p<0.05, **p<0.01, unpaired t-test.

performed. Samples were tested at two doses (25 µg and 2.5 µg per egg) as described in Materials and Methods. **Fig. 7** shows the antiangiogenic property of compounds/fractions from seeds and the priority fractions from leaves.

Branching analysis revealed that two of the five compounds (SAE-C-OCF4-F2 to F5) tested were antiangiogenic (**Fig. 8A**). Niazimicin (SAE-C-OCF4-F5) and SAE-C-OCF4-F3 were active at both concentrations, while niazirin (SAE-C-OCF4-F2) was anti–angiogenic at 25 µg only. These compounds exhibited no cytotoxicity against all cell lines tested, including MDCK normal kidney cells, demonstrating their ability to target specific biomolecules for angiogenesis without harming the normal cells.

Out of the ten open column fractions from leaves (ULOE-OCFs), five were anti–angiogenic at 25 µg. These are OCF3, OCF4, OCF6, OCF9, and OCF10 (**Fig. 8B**). OCF9 and OCF10 are the most promising showing antiangiogenic activity without cytotoxicity on MDCK normal kidney cells, while OCF3, OCF4 and OCF6 display antiproliferative activity in cancer cells, as well as on MDCK normal cells. It is noteworthy that OCF4 and OCF10 also have antimigration activity. This selective activity against migration and angiogenesis, two important hallmarks of cancer, provides a rationale for pursuing OCF10 as the active ingredient for the syrup formulation studies.

Compounds and fractions that are active in the CAM assay could be targeting various biomolecules that are specific to the inhibition of angiogenesis. A possible target could be vascular endothelial growth factor (VEGF) which, when inhibited, results in the inhibition of endothelial cell growth. VEGF is highly specific for endothelial cells; its binding to tyrosine kinase receptors results in endothelial cell proliferation, migration, and new blood vessel formation (Hoeben et al. 2004). Experiments to determine the mechanism of action of the actives, e.g., targeting VEGF, are recommended.

2.5. *Antioxidant Response Elements (ARE) activation and inhibition*

The *Nrf2* gene is expressed constitutively in the cell, transcribed into mRNA, and translated into the Nrf2 protein. In response to a trigger, Nrf2 protein gets translocated into the nucleus, where Nrf2 binds to ARE, activating several downstream genes (e.g., *GstA2*, *Nqo1*) involved in response to oxidative stress. Nrf2 gets targeted for ubiquitylation and degradation by Keap1 transiently shuttled into the nucleus. (Kobayashi et al. 2004, Ma 2013, Taguchi & Yamamoto 2017, Hayes & McMahon 2006) ARE inducers inhibit the Nrf2-Keap1 interaction, thereby allowing the Nrf2 protein to remain accessible for binding to ARE for a longer period of time, which in turn can lead to the upregulation of oxidative stress response genes activated by ARE (Nguyen et al. 2005). The activation of the Nrf2-ARE pathway is a known cancer-preventive strategy, exemplified by the natural product sulforaphane, a constituent of broccoli (Surh 2003). Enhancement of Nrf2 activity in cancer cells leads to proliferation and tissue invasion and has been linked to drug resistance, (Hayes & McMahon 2006, Shibata et al. 2008) hence inhibitors of the Nrf2 pathway (e.g., brusatol) are also useful in cancer treatment and in combination therapy.

ARE induction is measured using the ARE activation luciferase assay described by Ratnayake et al. (2013) and Matthews et al. (2018).

Extracts, partitions, and fractions prioritized for their cytotoxic activity were tested for ARE activation (**Fig. 9**). SAE-C (seeds, air-dried, ethanol extract, chloroform partition) showed modest ARE activity. From SAE-C, SAE-C-OCF4, and SAE-C-OCF5 caused the highest ARE activation in LNCaP prostate cancer cells. SAE-C-OCF3 also had high ARE activity, with greater activity at 1 µg/mL than at 100 µg/mL. Pooled SAE-C-OCF4 and OCF5 showed dose-dependent ARE activity at 100 µg/mL and 1 µg/mL. SAE-E-OCF4, one of the priority fractions, induced ARE activation at 100 µg/mL. The pooled SAE-C-OCF4 and OCF5 and their parent partition SAE-C also caused ARE activation at 100 µg/mL in MDA-MB-231 breast cancer cells. We mainly used the latter cell type to determine potential Nrf2/ARE inhibitory effects as MDA-MB-231 cells have a high basal activation level, and we identified some fractions that reduced the reporter signal; however, this was likely due to reduced cell viability.

At 100 µg/mL, most of the leaf fractions showed high ARE activation in LNCaP cells, most notably LOE-OCF10 (12.47 fold ARE activity). This fraction showed dose-dependent activity. ARE activation by LOE-OCF10 was used as one basis for prioritizing ULOE-OCF10 for the herbal syrup preparation, since LOE-OCF10 from small scale extraction and ULOE-OCF10 from upscale extraction have close to identical chemical profiles (**SI Fig. 4AB**). On the other hand, pooled LOE-OCF5 and OCF6 were ARE-activating at 10 µg/mL, but not at the higher concentration. Significant ARE activation by leaf extracts and fractions point to a great potential for leaf extract-based, non-cytotoxic herbal syrup formulations to be utilized for cancer chemoprotection.

3. Herbal syrup formulation

3.1. *Physicochemical properties*

Among the ULOE-OCFs, ULOE-OCF10 showed significant yield, selective cytotoxicity to SKOV-3 ovarian cancer cells and no cytotoxicity to MDCK normal cells, no apoptotic activity, antimigration activity, antiangiogenesis activity and its equivalent small-scale fraction LOE-OCF10 showed antioxidant activity. Hence, it was used as the prototype fraction for herbal syrup formulation (**Table 1**). One hundred (100) µg/mL of the ULOE-OCF10 or approximately 3X its potency or IC_{50} in SKOV-3 ovarian cancer cells was added to the syrup formulations as the bioactive component. The pH of the samples ranged from 6.14 to 6.77. The sweet taste and the bittersweet smell were virtually the same throughout the study period. No precipitation was observed in any of the samples within 14 days of storage at room temperature. White flocculence became visible on the 19th day for samples stored at room temperature but not on samples stored at the refrigerator or 4°C. This flocculence may be due to bacterial growth, which can be easily avoided by adding a sterilization step during the preparation of the herbal syrup. **Table 3** shows the physicochemical properties observed in the formulated herbal syrups.

Table 3: Physicochemical parameters of the formulated herbal syrups

Color	Pale Yellow
Odor	Bittersweet
Taste	Sweet
pH	6.14-6.77

3.2. *Cytotoxicity of ULOE-OCF10 herbal syrup*

To determine the stability of the active ingredient in the final product, herbal syrup formulations were tested for cytotoxicity in MTT assay. **Fig. 10** shows the MTT assay result of the formulations with and without the active extract on SKOV-3 ovarian and MDCK normal kidney cell lines. Cytotoxic activity was retained in syrup formulations 1, 2 and 4 with ULOE-OCF10 at 100 µg/mL, with 4 showing the highest cytotoxicity against ovarian cancer cells, suggesting that the ratio of the excipients used for formulation 4 is the most effective in conserving the active components of the extract. All formulations showed no cytotoxicity to ovarian cancer cells indicating that the simple syrup and the excipients used do not contribute to the observed cytotoxicity of the final products. More importantly, all formulations have very low toxicity (~5%) on normal kidney cells, showing consistent selectivity in ovarian cancer cells.

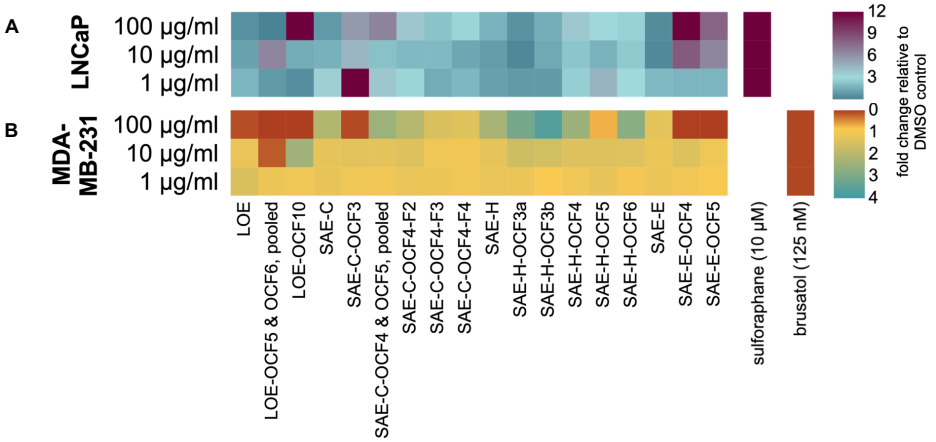

Figure 9: Antioxidant Response Element (ARE) (A) activation in LNCaP and (B) inhibition in MDA-MB-231 ARE-luc cells of fractions from seeds and leaves. Fold change ARE activation per unit cell of fractions from the seeds and leaves in LNCaP and MDA-MB-231 cells. High fold change (>5) in LNCaP cells indicate ARE activation while low fold change (<1) in MDA-MB-231 cells indicate ARE inhibition. Sulforaphane (10 µM) and brusatol (125 nM) were used as positive controls for ARE activation and inhibition, respectively.

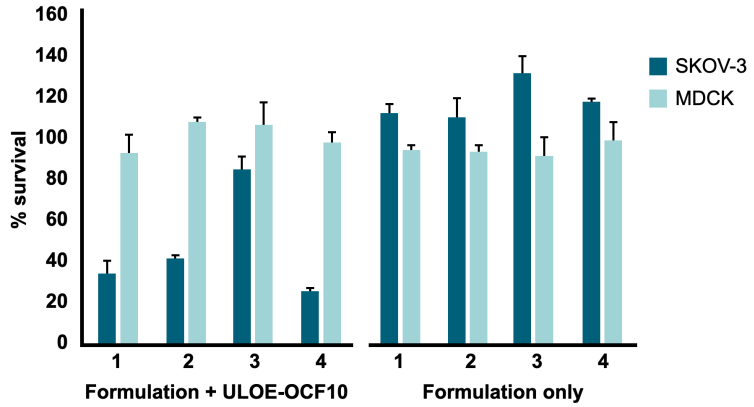

Figure 10: Antiproliferation of the herbal syrup formulations for ULOE-OCF10. SKOV-3 ovarian and MDCK normal kidney cells were treated either with the formulation alone or the formulation with 100 µg/mL ULOE-OCF10 for 72 h and the % survival was evaluated using MTT assay. Each bar represents mean ± SD tested in quadruplicates.

Here we demonstrate that an *M. oleifera* leaf extract can be formulated into a simple syrup without losing its activity *in vitro*. For further development, other experiments, e.g., identify more major compounds present in the active extract, determine their chemical stability at different time intervals, conduct dose-response experiments for the herbal syrup *in vitro* and *in vivo*; perform microbial stability testing, determine long-term stability (>6 months) at room temperature and under refrigeration, are recommended.

CONCLUSIONS

This study presents the isolation and determination of nitrile and O-thiocarbamate glycosides from the seeds of *M. oleifera* (**SI Table 12)**, corroborating previous extractions of these compounds from the same plant (Faizi et al. 1992, Guevara et al. 1999). Certain compounds and fractions showed inhibitory activity in assays corresponding to the hallmarks of cancer, i.e., cell proliferation, evasion of apoptosis, invasion and metastasis, and angiogenesis. Previous studies report that seed extracts from *M. oleifera* attenuate oxidative stress (Flora and Pachauri 2011), allowing the seeds to adapt and tolerate inhospitable conditions during germination (Boumenjel et al. 2021).

We used the mature leaves to prepare syrup formulations from *M. oleifera*. Leaves present a sustainable and highly yielding food source; i.e., harvest of these parts will not terminate the plant's life. Studies show that compounds in *Moringa* leaves mitigate oxidative and salinity-induced stress in the *Moringa* plant, aiding it in its survival (Azam et al. 2020, Hassan et al. 2020, Howladar 2014).

We formulated a syrup from ULOE-OCF10 at 3x its IC_{50} in ovarian cancer cells. The formulated syrup suppressed ovarian cancer cell proliferation and did not suppress normal human kidney cell growth. The formula remained soluble and preserved its taste throughout the 28 days of observation, and flocculence was avoided by refrigeration. MS evidence identifies flavonoids, lipids and derivatives, and a tetrapyrrole, present in ULOE-OCF10 with previously reported antioxidant, cancer preventive and antiproliferative properties. The study provides additional evidence of *M. oleifera*'s cancer chemoprotective properties, i.e. activation of antioxidant response elements, and thus its potential for development as a nutraceutical herbal product.

ACKNOWLEDGMENTS

This research entitled "*Malunggay-derived Antitumor Compounds: Isolation, Characterization, Bioactivity and Molecular Targets"* was one of several projects under the Philippine Department of Science and Technology-Philippine Council for Health Research and Development (DOST-PCHRD) program entitled TERRAPHARMA: Nutritional, Therapeutic and Prophylactic Properties of *Moringa oleifera* Lam. We thank Dr. Hiyas A. Junio of the Mass Spectrometry Facility, Institute of Chemistry, U.P. Diliman for guidance on mass spectrometry and molecular networking analysis of ULOE-OCF10. The ARE assays were supported by the Debbie and Sylvia DeSantis Chair professorship (H.L.). We thank Dr. Donna Zhang for supplying the MDA-MB-231 ARE-luc reporter cell line.

This manuscript is dedicated to the late Congressman Luis R. Villafuerte who was one of the staunchest champions of Science and Technology, Research and Development, in the Philippines. He had a specific interest in the development of herbal products from *Moringa oleifera* and strongly encouraged U.P. researchers to pursue studies on the nutritional, medicinal, curative and chemopreventive properties of *Moringa*.

CONFLICT OF INTEREST

Intellectual property protection is being filed by the authors for results reported in this manuscript.

CONTRIBUTIONS OF INDIVIDUAL AUTHORS

JMML performed experiments to extract, purify, characterize and identifiy compounds from *Moringa* samples, performed NMR experiments, prepared and characterized the herbal syrup formulation, analyzed the data and results, and wrote the paper.

MRDP collected and processed *Moringa* leaf and seed samples, extracted and purified *Moringa* samples, designed and performed MTT cell viability/cytotoxicity and Matrigel antimigration experiments, analyzed the data and results, and wrote the paper.

ALL designed and performed the *in ovo* CAM antiangiogenesis and MTT-based cell viability/cytotoxicity experiments, and analyzed the data and results.

JOT designed and performed the flow cytometry apoptosis experiments and analyzed the data and results.

CMVR compiled all the methods, data and results, analyzed the data and results, prepared the tables and figures, and wrote the paper.
KFVR performed the mass spectrometry experiments and analyzed the data and results.

MOC and ELB collected and processed *Moringa* leaf and seed samples.
HL, RR and JHM contributed the ARE-luciferase results.

LASR analyzed the data and results from all experiments, and wrote the paper.

GPC served as project leader, conceptualized and designed the project, led its implementation, supervised the researchers and experiments, evaluated the data and results from all experiments, and wrote the paper.

REFERENCES

Abassi, Y.A., Xi, B., Zhang, W., Ye, P., Kirstein, S.L., Gaylord, M.R., Feinstein, S.C., Wang, X., & Xu, X. 2009. Kinetic cell-based morphological screening: prediction of mechanism of compound action and off-target effects. *Cell Chem Bio, 16*, 712-723.

Atolani, O., Olorundare, O.E., Banerjee P., Osin, O. A. Preissner, R., and Njan. A. A. "Isolation, characterisation and in silico toxicity evaluations of thiocarbamates, isothiocyanates, nitrile, glucosinolate and lipids from Moringa oleifera Lam. seed." *Journal of the Turkish Chemical Society Section A: Chemistry* 7, no. 1 (2020): 233-242.

Azam, S., Nouman, W., Rehman, U.U., Ahmed, U., Gull, T. and Shaheen, M., 2020. Adaptability of Moringa oleifera Lam. under different water holding capacities. *South African Journal of Botany*, *129*, pp.299-303.

Babaei, F., Moafizad, A., Darvishvand, Z., Mirzababaei, M., Hosseinzadeh, H. and Nassiri-Asl, M., 2020. Review of the effects of vitexin in oxidative stress-related diseases. *Food science & nutrition*, *8*(6), pp.2569-2580.

Bhakkiyalakshmi, E., Sireesh, D. and Ramkumar, K.M., 2018. Redox Sensitive transcription via Nrf2-Keap1 in suppression of inflammation. In *Immunity and Inflammation in Health and Disease* (pp. 149-161). Academic Press.

Boumenjel, A., Pantera, A., Papadopoulos, A. and Ammari, Y., 2021. Tolerance and adaptation mechanisms developed by Moringa oleifera (L) seeds under oxidative stress induced by salt stress during in vitro germination. *Global NEST Journal*, *23*(1), pp.152-161.

Burdick, J.D., Gao, Y., Kanengiser, B., Merrill, J.C. and Harbell, J.W., 2003. Comparative assessment of two eye area cosmetic formulations through evaluation of alternative eye irritation methods relative to endpoints measured in a human clinical subacute study design. *The Toxicologist*, *72*(S1), p.220.

Comşa, Ş., Cimpean, A.M. and Raica, M., 2015. The story of MCF-7 breast cancer cell line: 40 years of experience in research. *Anticancer research*, *35*(6), pp.3147-3154.

de Los Reyes, C., Ortega, M.J., Rodriguez-Luna, A., Talero, E., Motilva, V. and Zubia, E., 2016. Molecular characterization and antiinflammatory activity of galactosylglycerides and galactosylceramides from the microalga Isochrysis galbana. *Journal of agricultural and food chemistry*, *64*(46), pp.8783-8794.

di Camillo Orfali, G., Duarte, A.C., Bonadio, V., Martinez, N.P., De Araújo, M.E.M.B., Priviero, F.B.M., Carvalho, P.O. and Priolli, D.G., 2016. Review of anticancer mechanisms of isoquercitin. *World journal of clinical oncology*, *7*(2), p.189.

Dixelius, J., Larsson, H., Sasaki, T., Holmqvist, K., Lu, L., Engström, A., Timpl, R., Welsh, M. and Claesson-Welsh, L., 2000. Endostatin-induced tyrosine kinase signaling through the Shb adaptor protein regulates endothelial cell apoptosis. *Blood, The Journal of the American Society of Hematology*, *95*(11), pp.3403-3411.

Fahey, J.W., Olson, M.E., Stephenson, K.K., Wade, K.L., Chodur, G.M., Odee, D., Nouman, W., Massiah, M., Alt, J., Egner, P.A. and Hubbard, W.C., 2018. The diversity of chemoprotective glucosinolates in Moringaceae (Moringa spp.). *Scientific reports*, *8*(1), pp.1-14.

Fahey, J.W., Wade, K.L., Stephenson, K.K., Shi, Y., Liu, H., Panjwani, A.A., Warrick, C.R. and Olson, M.E., 2019. A strategy to deliver precise oral doses of the glucosinolates or isothiocyanates from moringa oleifera leaves for use in clinical studies. *Nutrients*, *11*(7), p.1547.

Faizi, S., Siddiqui, B.S., Saleem, R., Siddiqui, S. and Aftab, K., 1992. Novel hypotensive agents, niazimin A, niazimin B, niazicin A and niazicin B from *Moringa oleifera*: Isolation of first naturally occurring carbamates. *Journal of the Chemical Society, Perkin Transactions 1*, (20), pp.3035-3040.

Faizi, S., Siddiqui, B.S., Saleem, R., Noor, F. and Husnain, S., 1997. Isolation and structure elucidation of a novel glycoside niazidin from the pods of Moringa oleifera. *Journal of Natural Products*, *60*(12), pp.1317-1321.

Flora, S.J. and Pachauri, V., 2011. Moringa (Moringa oleifera) seed extract and the prevention of oxidative stress. In *Nuts and seeds in health and disease prevention* (pp. 775-785). Academic Press.

Guevara, A.P., Vargas, C., Sakurai, H., Fujiwara, Y., Hashimoto, K., Maoka, T., Kozuka, M., Ito, Y., Tokuda, H. and Nishino, H., 1999. An antitumor promoter from Moringa oleifera Lam. *Mutation Research/Genetic Toxicology and Environmental Mutagenesis*, *440*(2), pp.181-188.

Hanahan, D. and Weinberg, R.A., 2011. Hallmarks of cancer: the next generation. *cell*, *144*(5), pp.646-674.

Hassan, F., Al-Yasi, H., Ali, E., Alamer, K., Hessini, K., Attia, H. and El-Shazly, S., 2020. Mitigation of salt-stress effects by moringa leaf extract or salicylic acid through motivating antioxidant machinery in damask rose. *Canadian Journal of Plant Science*, *101*(2), pp.157-165.

Hayes, J.D. and McMahon, M., 2006. The double-edged sword of Nrf2: subversion of redox homeostasis during the evolution of cancer. *Molecular cell*, *21*(6), pp.732-734.

Hertog, M.G., Hollman, P.C., Katan, M.B. and Kromhout, D., 1993. Intake of potentially anticarcinogenic flavonoids and their determinants in adults in The Netherlands.

Howladar, S.M., 2014. A novel Moringa oleifera leaf extract can mitigate the stress effects of salinity and cadmium in bean (Phaseolus vulgaris L.) plants. *Ecotoxicology and Environmental Safety*, *100*, pp.69-75.

Huang, L., Yuan, C. and Wang, Y., 2020. Bioactivity-guided identification of antiadipogenic isothiocyanates in the moringa (Moringa oleifera) seed and investigation of the structure-activity relationship. *Molecules*, *25*(11), p.2504.

Kamal, M.M., Akter, S., Lin, C.N. and Nazzal, S., 2020. Sulforaphane as an anticancer molecule: mechanisms of action, synergistic effects, enhancement of drug safety, and delivery systems. *Archives of pharmacal research*, *43*(4), pp.371-384.

Kobayashi, A., Kang, M.I., Okawa, H., Ohtsuji, M., Zenke, Y., Chiba, T., Igarashi, K. and Yamamoto, M., 2004. Oxidative stress sensor Keap1 functions as an adaptor for Cul3-based E3 ligase to regulate proteasomal degradation of Nrf2. *Molecular and cellular biology*, *24*(16), pp.7130-7139.

Kotecha, R., Takami, A. and Espinoza, J.L., 2016. Dietary phytochemicals and cancer chemoprevention: a review of the clinical evidence. *Oncotarget*, *7*(32), p.52517.

Kikuchi, A., Nieda, M., Schmidt, C., Koezuka, Y., Ishihara, S., Ishikawa, Y., Tadokoro, K., Durrant, S., Boyd, A., Juji, T. and Nicol, A., 2001. In vitro antitumour activity of α-galactosylceramide-stimulated human invariant Vα24+ NKT cells against melanoma. *British journal of cancer*, *85*(5), pp.741-746.

Kluska, M., Juszczak, M., Żuchowski, J., Stochmal, A. and Woźniak, K., 2021. Kaempferol and its glycoside derivatives as modulators of etoposide activity in HL-60 cells. *International Journal of Molecular Sciences*, *22*(7), p.3520.

Langner, E., & Rzeski, W. (2012). Dietary derived compounds in cancer chemoprevention. *Contemporary Oncology*, *16*(5), 394.

Lee, T.J., Kim, O.H., Kim, Y.H., Lim, J.H., Kim, S., Park, J.W. and Kwon, T.K., 2006. Quercetin arrests G2/M phase and

induces caspase-dependent cell death in U937 cells. *Cancer letters*, *240*(2), pp.234-242.

Liang, C.C., Park, A.Y., & Guan, J.L. 2007. *In vitro* scratch assay: a convenient and inexpensive method for analysis of cell migration *in vitro*. *Nature protocols, 2*(2), 329-333.

Loeb, L.A. and Harris, C.C., 2008. Advances in chemical carcinogenesis: a historical review and prospective. *Cancer research*, *68*(17), p.6863.

Lokman, N.A., Elder, A.S., Ricciardelli, C. and Oehler, M.K., 2012. Chick chorioallantoic membrane (CAM) assay as an in vivo model to study the effect of newly identified molecules on ovarian cancer invasion and metastasis. *International journal of molecular sciences*, *13*(8), pp.9959-9970.

Ma, Q., 2013. Role of nrf2 in oxidative stress and toxicity. *Annual review of pharmacology and toxicology*, *53*, p.401.

Matthews, J.H., Liang, X., Paul, V.J. and Luesch, H., 2018. A complementary chemical and genomic screening approach for druggable targets in the Nrf2 pathway and small molecule inhibitors to overcome cancer cell drug resistance. *ACS chemical biology*, *13*(5), pp.1189-1199.

Martin, K. 2006. Targeting Apoptosis with Dietary Bioactive Agents. *Exp Biol Med, 231*, 117–129.

Maurya, A., Gupta, S. and Srivastava, S.K., 2011. Preparative isolation of bioactive nitrile glycoside "Niazirin" from the fruits of Moringa oleifera using fast centrifugal partition chromatography. *Separation Science and Technology*, *46*(7), pp.1195-1199.

Meireles, D., Gomes, J., Lopes, L., Hinzmann, M. and Machado, J., 2020. A review of properties, nutritional and pharmaceutical applications of Moringa oleifera: integrative approach on conventional and traditional Asian medicine. *Advances in Traditional Medicine*, *20*(4), pp.495-515.

Michael, M. and Doherty, M.M., 2005. Tumoral drug metabolism: overview and its implications for cancer therapy. *Journal of Clinical Oncology*, *23*(1), pp.205-229.

Molecular Probes, Inc. 2010. *Manual for FITC Annexin V/Dead Cell Apoptosis Kit with FITC annexin V and PI, for Flow Cytometry Catalog no. V13242.* Retrieved June 25, 2014, from Life Technologies: http://tools.lifetechnologies.com/content/sfs/manuals/mp13242.pdf

Molino, R.J.E.J., Rellin, K.F.B., Nellas, R.B. and Junio, H.A., 2021. Small in size, big on taste: Metabolomics analysis of flavor compounds from Philippine garlic. *PloS one*, *16*(5), p.e0247289.

Mosmann, T. 1983. Rapid colorimetric assay for cellular growth and survival: application to proliferation and cytotoxicity assays. *J Immunol Methods , 65* (1-2), 55-63.

Murakami A, Kitazono Y, Jiwajinda S, et al. 1998. Niaziminin, a Thiocarbamate from the Leaves of Moringa oleifera, holds a Strict Structural Requirement for Inhibition of Tumor-Promoter-Induced Epstein-Barr Virus Activation. Planta Med 64(4):319-323.

Nakagawa, R., Serizawa, I., Motoki, K., Sato, M., Ueno, H., Iijima, R., Nakamura, H., Shimosaka, A. and Koezuka, Y., 2001. Antitumor activity of α-galactosylceramide, KRN7000, in mice with the melanoma B16 hepatic metastasis and immunohistological study of tumor infiltrating cells. *Oncology Research Featuring Preclinical and Clinical Cancer Therapeutics*, *12*(2), pp.51-58.

Ngelangel, C., & Wang, A. 2002. Cancer and the Cancer Philippine Control Program. *Jpn J Clin Oncol , 32* (Supplement 1), S52-S61.

Nguyen, T., Nioi, P. and Pickett, C.B., 2009. The Nrf2-antioxidant response element signaling pathway and its activation by oxidative stress. *Journal of biological chemistry*, *284*(20), pp.13291-13295.

Niazi, S.K., 2019. *Handbook of Pharmaceutical Manufacturing Formulations: Liquid Products*. CRC Press.

Olayanju, A., Copple, I.M., Bryan, H.K., Edge, G.T., Sison, R.L., Wong, M.W., Lai, Z.Q., Lin, Z.X., Dunn, K., Sanderson, C.M. and Alghanem, A.F., 2015. Brusatol provokes a rapid and transient inhibition of Nrf2 signaling and sensitizes mammalian cells to chemical toxicity—implications for therapeutic targeting of Nrf2. *Free Radical Biology and Medicine*, *78*, pp.202-212.

Oluduro et al. 2012. Evaluation of Antibacterial Potential of Crude Extract of *Moringa Oleifera* seed on Orthopaedics Wound Isolates and Characterization of Phenylmethanamine and Benzyl Isothiocyanate Derivatives. *Research Journal of Medicinal Plant*.

Raga, D.D., Alimboyoguen, A.B., Shen, C.C., Herrera, A.A. and Ragasa, C.Y., 2011. Triterpenoids and an antiangiogenic sterol from Ardisia pyramidalis (Cav.) Pers. *Philipp Agric Sci*, *94*(2), pp.103-110.

Ragasa, C.Y., Levida, R.M., Don, M.J. and Shen, C.C., 2012. Cytotoxic isothiocyanates from Moringa oleifera Lam seeds. *Philipp. Sci. Lett*, *5*, pp.46-52.

Ragasa, C.Y., Ng, V.A.S. and Shen, C.C., 2016. Chemical constituents of Moringa oleifera Lam. seeds. *International Journal of Pharmacognosy and Phytochemical Research*, *8*(3), pp.495-498.

Ratnayake, R., Liu, Y., Paul, V.J. and Luesch, H., 2013. Cultivated sea lettuce is a multiorgan protector from oxidative and inflammatory stress by enhancing the endogenous antioxidant defense system. *Cancer Prevention Research*, *6*(9), pp.989-999.

Ren, D., Villeneuve, N.F., Jiang, T., Wu, T., Lau, A., Toppin, H.A. and Zhang, D.D., 2011. Brusatol enhances the efficacy of chemotherapy by inhibiting the Nrf2-mediated defense mechanism. *Proceedings of the National Academy of Sciences*, *108*(4), pp.1433-1438.

Riccardi, C., & Nicoletti, I. 2006. Analysis of apoptosis by propidium iodide staining and flow cytometry. *Nature protocols , 1* (3), 1458-1461.

Saleem, R. 1995. Studies in the chemical constituents of *Moringa Oleifer Lam.* Ph.D. thesis. University of Karachi, Karachi.

Saide, A., Lauritano, C. and Ianora, A., 2020. Pheophorbide a: State of the Art. *Marine Drugs*, *18*(5), p.257.

Shannon, P., Markiel, A., Ozier, O., Baliga, N.S., Wang, J.T., Ramage, D., Amin, N., Schwikowski, B. and Ideker, T., 2003. Cytoscape: a software environment for integrated models of biomolecular interaction networks. *Genome research*, *13*(11), pp.2498-2504.

Shen, K.H., Liao, A.C.H., Hung, J.H., Lee, W.J., Hu, K.C., Lin, P.T., Liao, R.F., and Chen, P.S. 2014. α-solanine inhibits invasion of human prostate cancer cell by suppressing epithelial-mesenchymal transition and MMPs expression. *Molecules, 19*, 11896-11914.

Shibata, T., Kokubu, A., Gotoh, M., Ojima, H., Ohta, T., Yamamoto, M. and Hirohashi, S., 2008. Genetic alteration of Keap1 confers constitutive Nrf2 activation and resistance to chemotherapy in gallbladder cancer. *Gastroenterology*, *135*(4), pp.1358-1368.

Shichiri, M. and Hirata, Y. 2001. Antiangiogenesis signals by endostatin. FASEB J. 1044 – 53.

Surh, Y.J., 2003. Cancer chemoprevention with dietary phytochemicals. *Nature Reviews Cancer*, *3*(10), pp.768-780.

Tacar, O., Sriamornsak, P., & Dass, C. R. 2013. Doxorubicin: an update on anticancer molecular action, toxicity and novel drug delivery systems. *J Pharm and Pharmacol, 65*(2), 157-170.

Taguchi, K. and Yamamoto, M., 2017. The KEAP1–NRF2 system in cancer. *Frontiers in oncology*, *7*, p.85.

Tan, X.L. and Spivack, S.D., 2009. Dietary chemoprevention strategies for induction of phase II xenobiotic-metabolizing enzymes in lung carcinogenesis: a review. *Lung cancer*, *65*(2), pp.129-137.

Van Wagenen, B., Larsen, R., Cardellina, J. I., Ran dazzo, D., Lidert, Z., & Swithenbank, C. 1993. Ulosantoin, a potent insecticide from the sponge Ulosa ruetzleri. *J Org Chem , 58*, 335-337.

Wang, K., Jiang, J., Lei, Y., Zhou, S., Wei, Y. and Huang, C., 2019. Targeting metabolic–redox circuits for cancer therapy. *Trends in biochemical sciences*, *44*(5), pp.401-414.

Wang, M., Carver, J.J., Phelan, V.V., Sanchez, L.M., Garg, N., Peng, Y., Nguyen, D.D., Watrous, J., Kapono, C.A., Luzzatto-Knaan, T. and Porto, C., 2016. Sharing and community curation of mass spectrometry data with Global Natural Products Social Molecular Networking. *Nature biotechnology*, *34*(8), pp.828-837.

Waris, G. and Ahsan, H., 2006. Reactive oxygen species: role in the development of cancer and various chronic conditions. *Journal of carcinogenesis*, *5*, p.14.

Yamaguguchi, H., Wyckoff, J., & Condeelis, J. 2005. Cell migration in tumors. *Curr Opin Cell Biol, 17*, 559-564.

Zhang Y. and Talalay P. 1994. Anticarcinogenic Activities of Organic Isothiocyanates: Chemistry and Mechanisms. The Johns Hopkins University School of Medicine. *Cancer Research.*

SUPPORTING INFORMATION

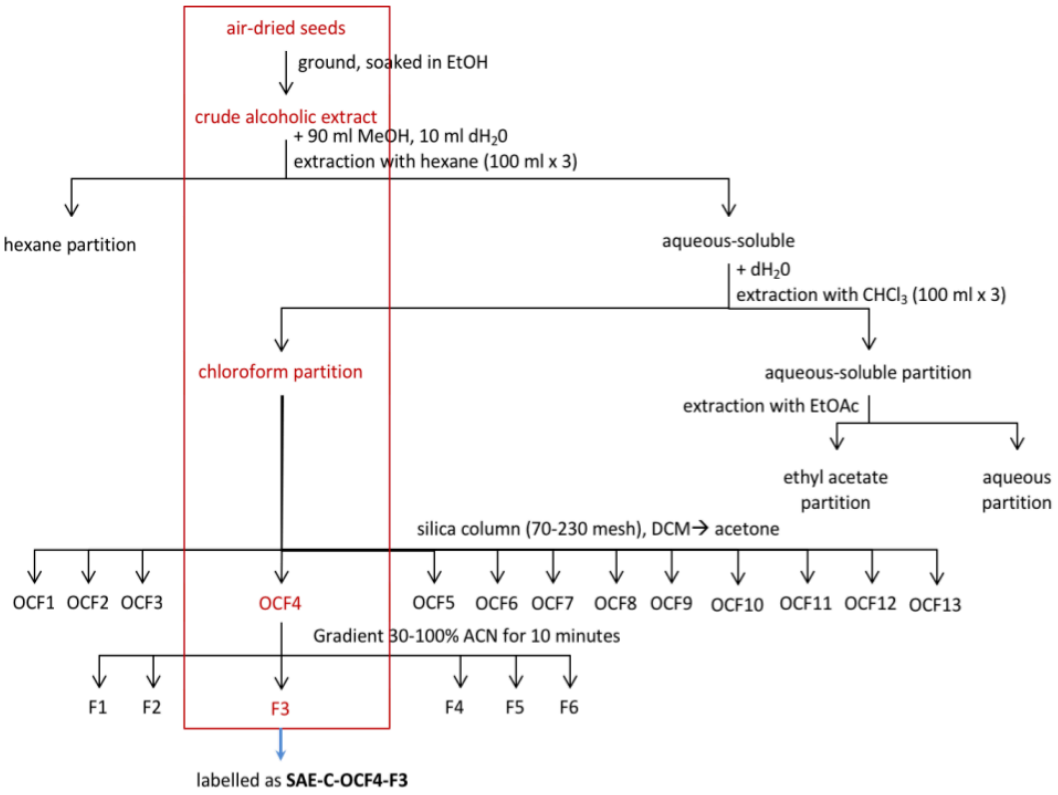

SI Figure 1: Labeling of samples in *Moringa* extraction and purification process

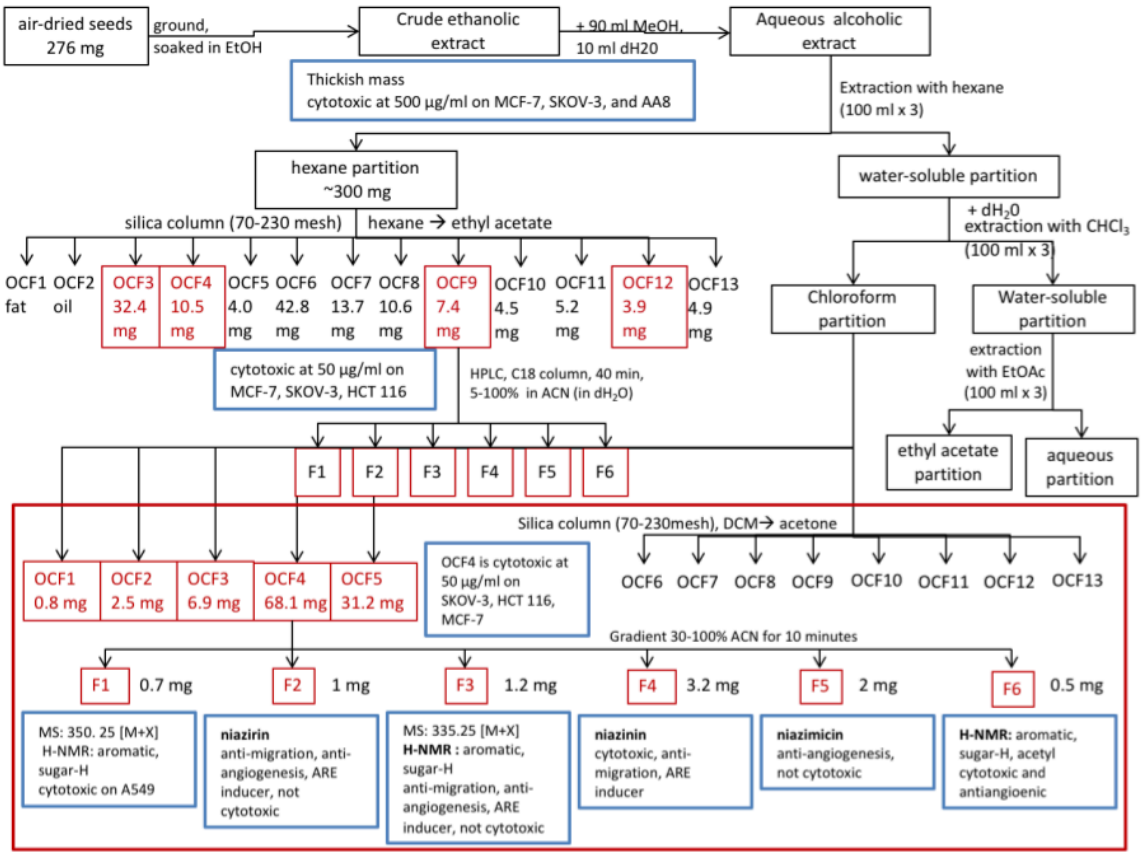

SI Figure 2: Purification of compounds from *Moringa* seeds (SAE – seeds, air-dried, ethanol)

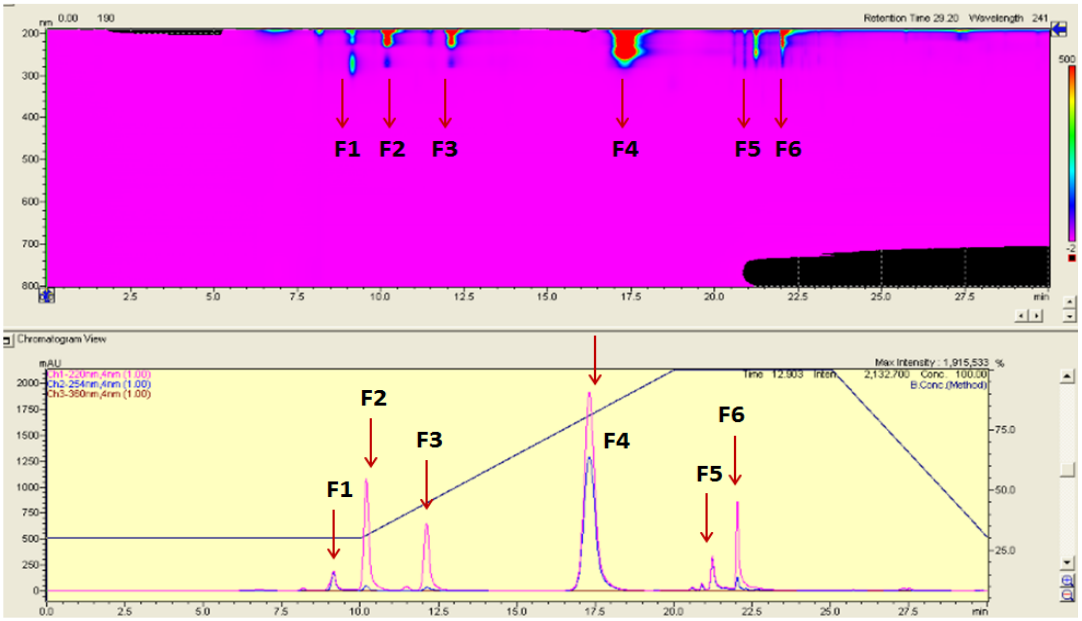

SI Figure 3: HPLC profile of SAE-C-OCF4 (open column fraction 4 from the chloroform partition of the ethanolic seed extract). Contour plot (top) and chromatogram (bottom) using semi-preparative C18 column. Approximately 12 mg was injected at a volume of 50-100 µl, and ran at a 30-100% ACN gradient for 10 mins with flow rate of 2 ml/min. Pink, blue, and brown chromatograms indicate absorbance at 220 nm, 254 nm and 360 nm, respectively.

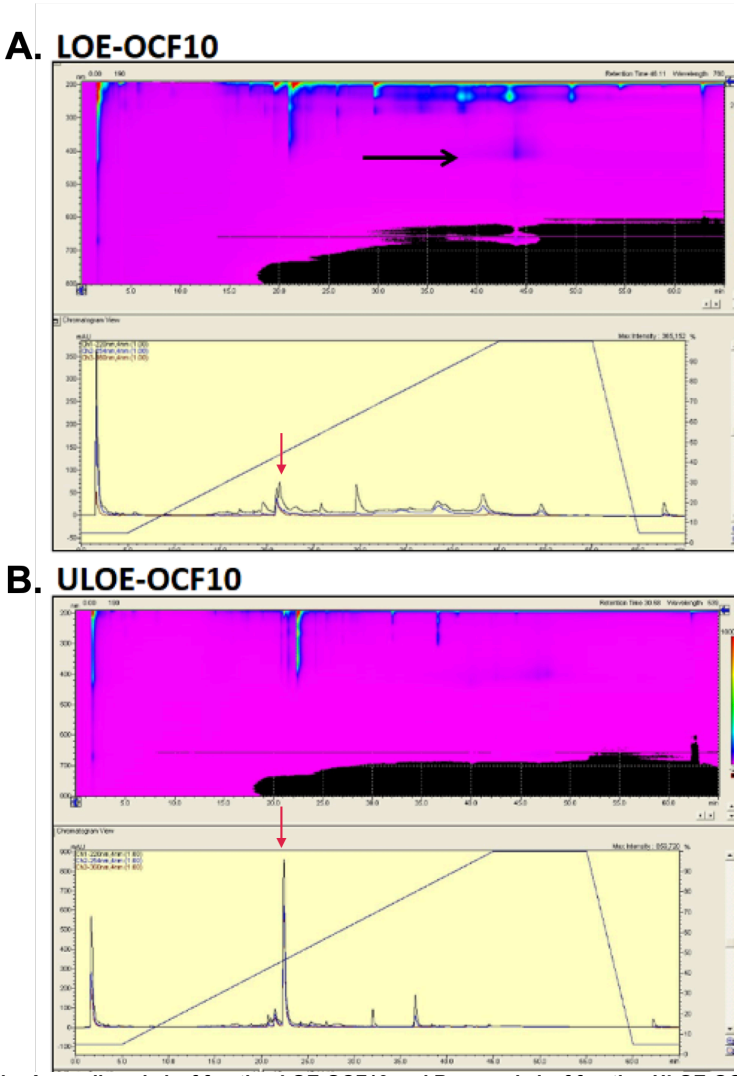

SI Figure 4: HPLC Profiles of the A. small-scale leaf fraction LOE-OCF10 and B. upscale leaf fraction ULOE-OCF10. Red arrow indicates the major compound, ULOE-OCF10-F1 and corresponding peak in LOE-OCF10. Samples were ran using an analytical C18 column at a 5-100% ACN gradient for 40 minutes with a flow rate of 1 ml/min. Black, blue, and brown chromatograms indicate absorbance at 220 nm, 254 nm and 360 nm, respectively.

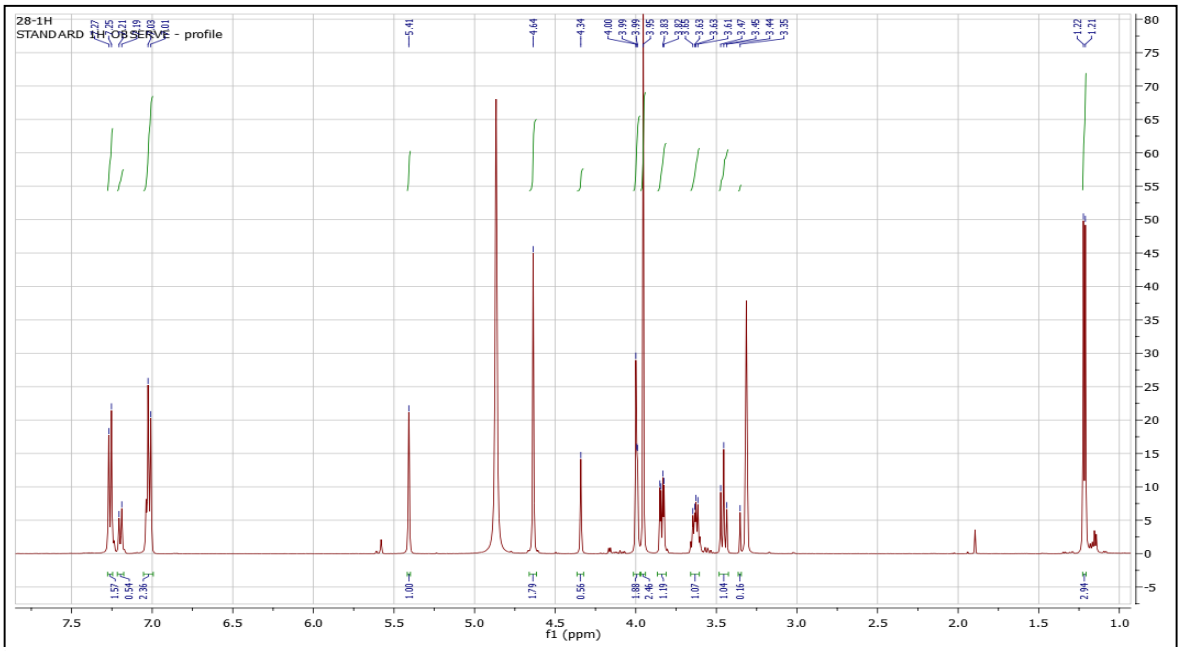

SI Figure 5A: ^{1}H-NMR spectral data of SAE-C-OCF 4-F4 (niazinin). Chemical shifts were recorded at 600 MHz with CD_3OD as solvent.

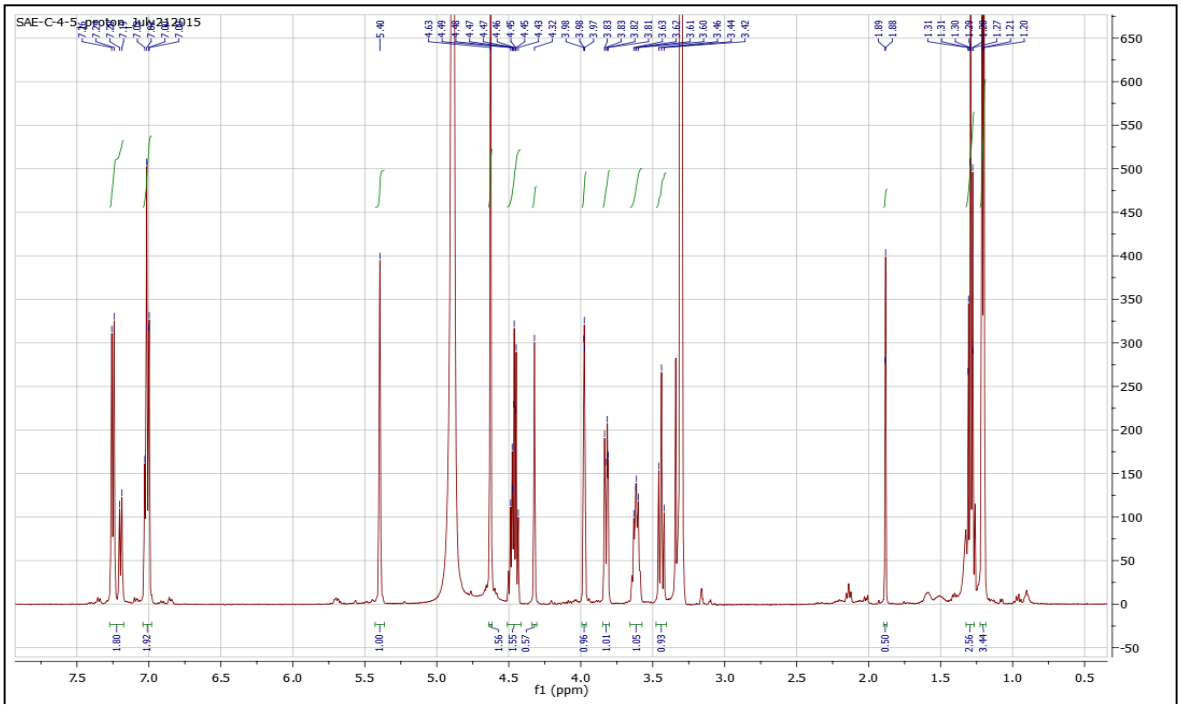

SI Figure 5B: ^{1}H-NMR spectral data of SAE-C-OCF4-F5 (niazimicin). Chemical shifts were recorded at 500 MHz with CD_3OD as solvent. Acquired from UP Diliman.

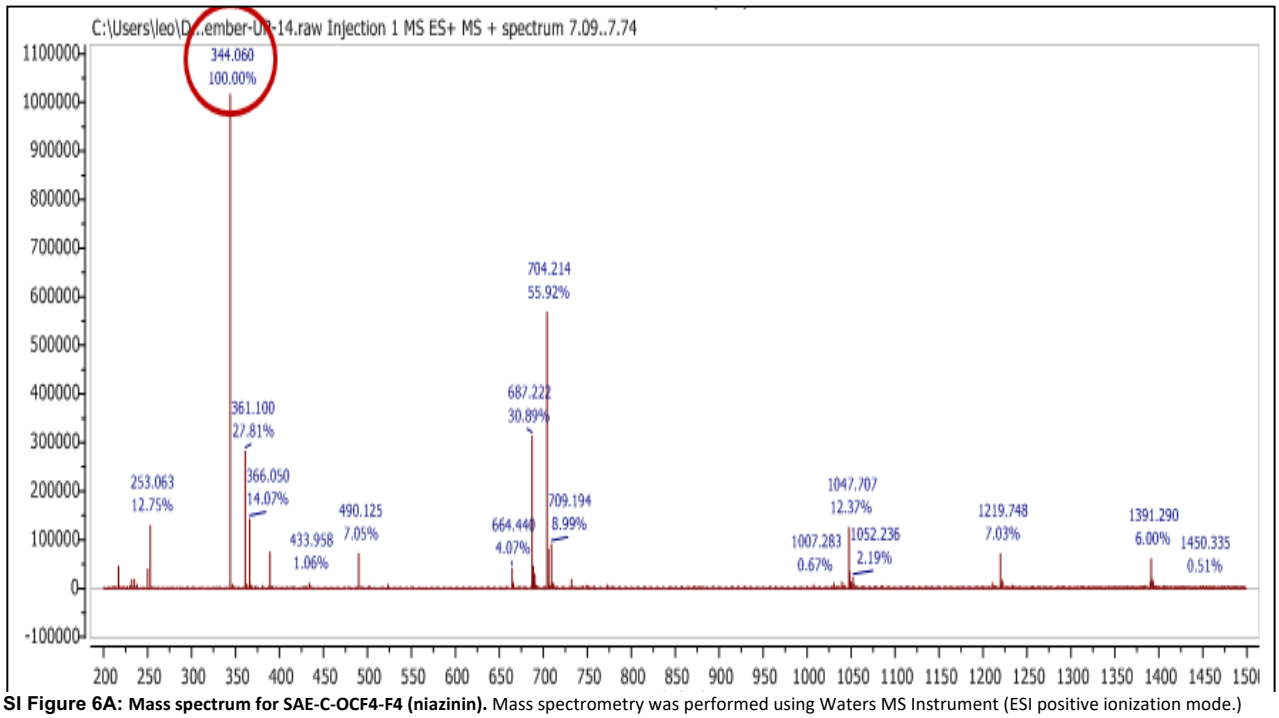

SI Figure 6A: Mass spectrum for SAE-C-OCF4-F4 (niazinin). Mass spectrometry was performed using Waters MS Instrument (ESI positive ionization mode.)

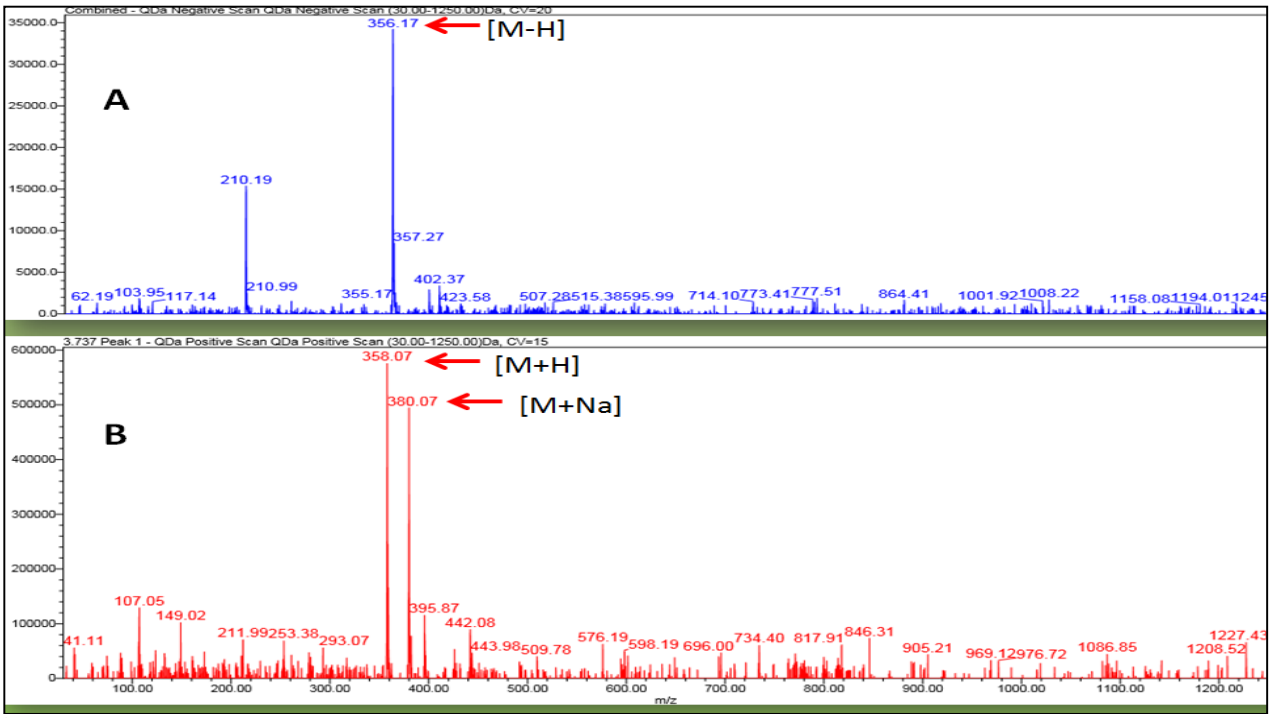

SI Figure 6B: Mass spectra of SAE-C-OCF4-F5 (niazimicin). Mass spectrometry was performed using ACQUITY UPLC MS by Waters in (A) ESI negative mode, and (B) ESI positive mode.

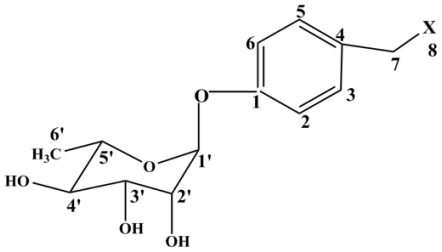

Niazinin X= NH-CS-OCH_3 (SAE-C-OCF4-F4)

Niazimicin X= NH-CS-OCH_2CH_3 (SAE-C-OCF4-F5)

SI Figure 7: Structure of niazinin and niazimicin

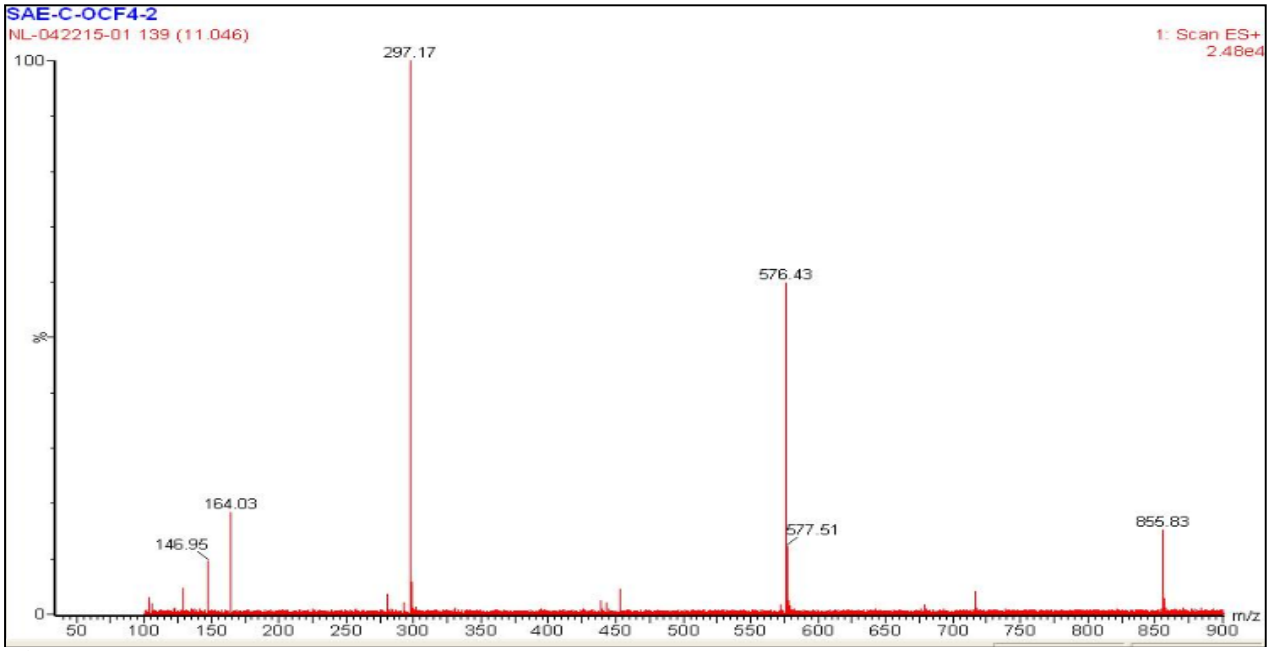

SI Figure 8A: Mass spectrum of SAE-C-OCF4-F2 (niazirin). Mass spectrometry was performed using Waters MS intrument (ESI positive ionization mode.)

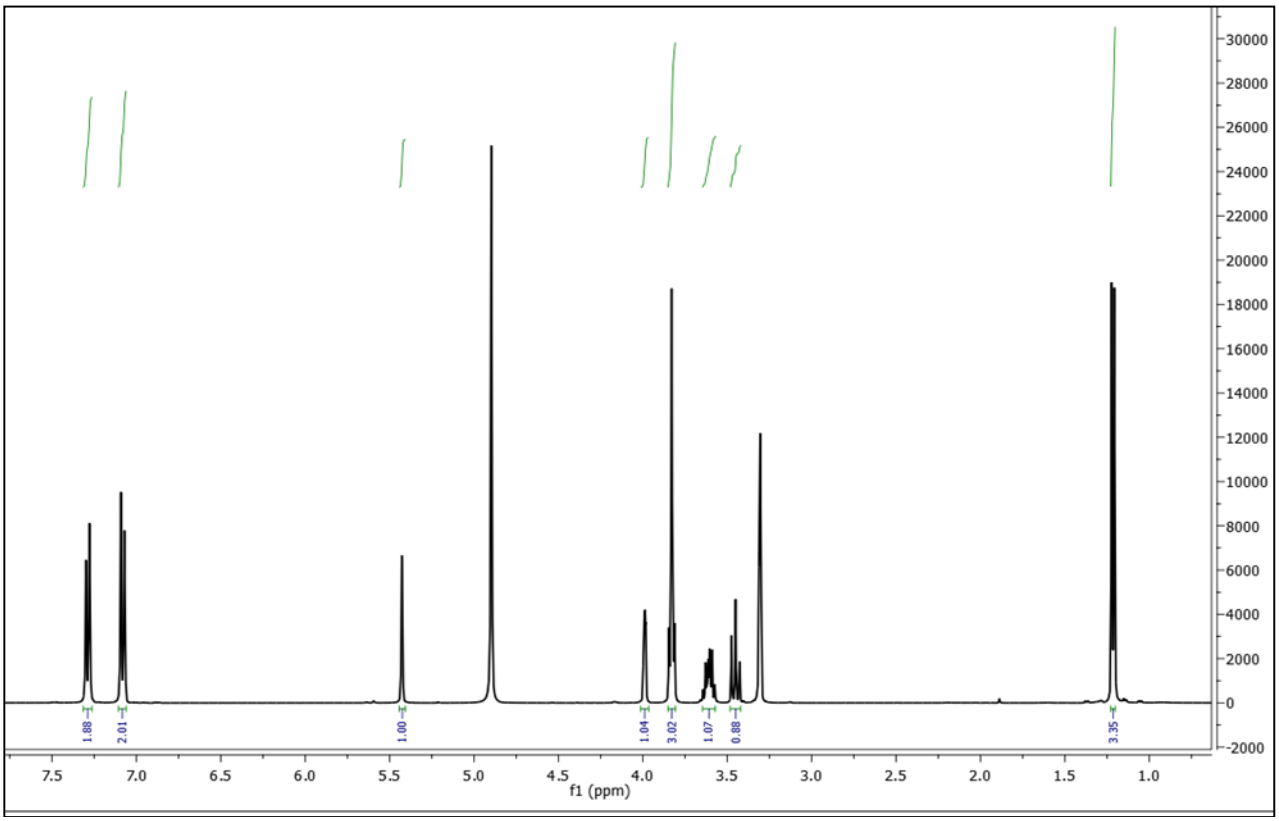

SI Figure 8B: ^{1}H-NMR spectral data of SAE-C-OCF4-F2 (niazirin). Chemical shifts were recorded at 500 MHz with CD_3OD as solvent. Acquired from UP Diliman.

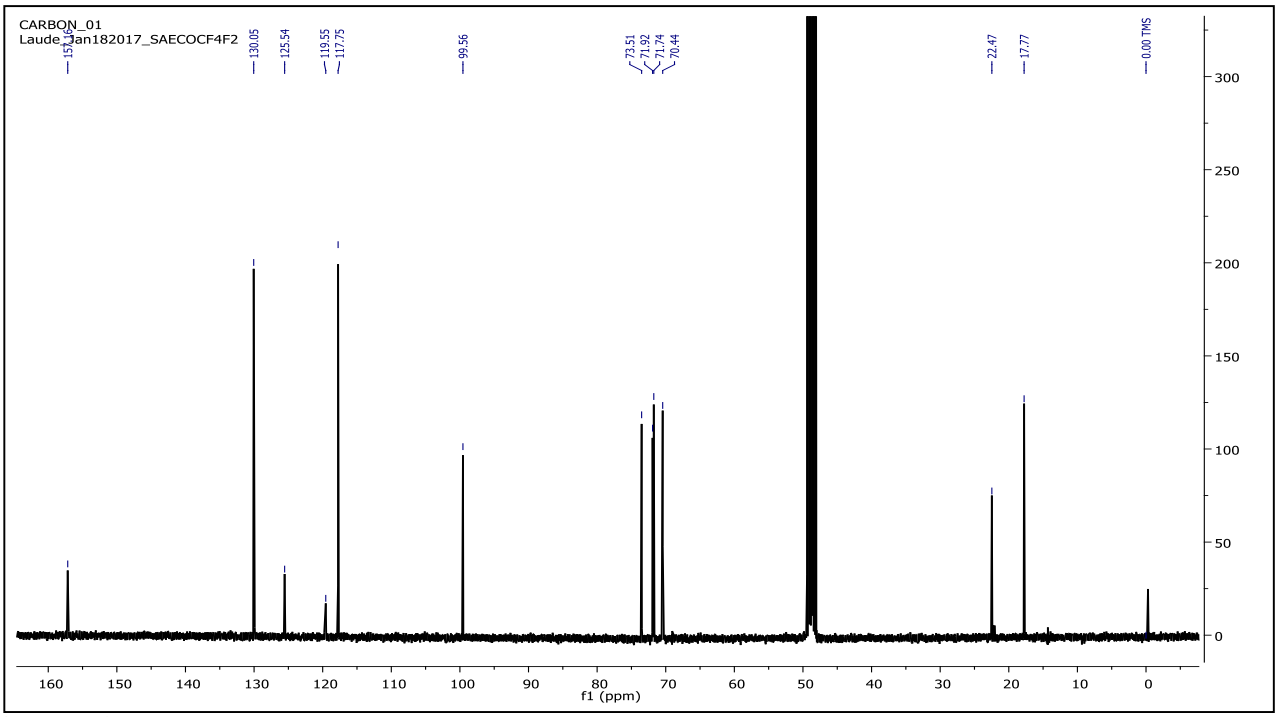

SI Figure 8C: ^{13}C-NMR of SAE-C-OCF4-F2 (niazirin). Chemical shifts were recorded at 500 MHz with CD_3OD as solvent. Acquired from UP Diliman.

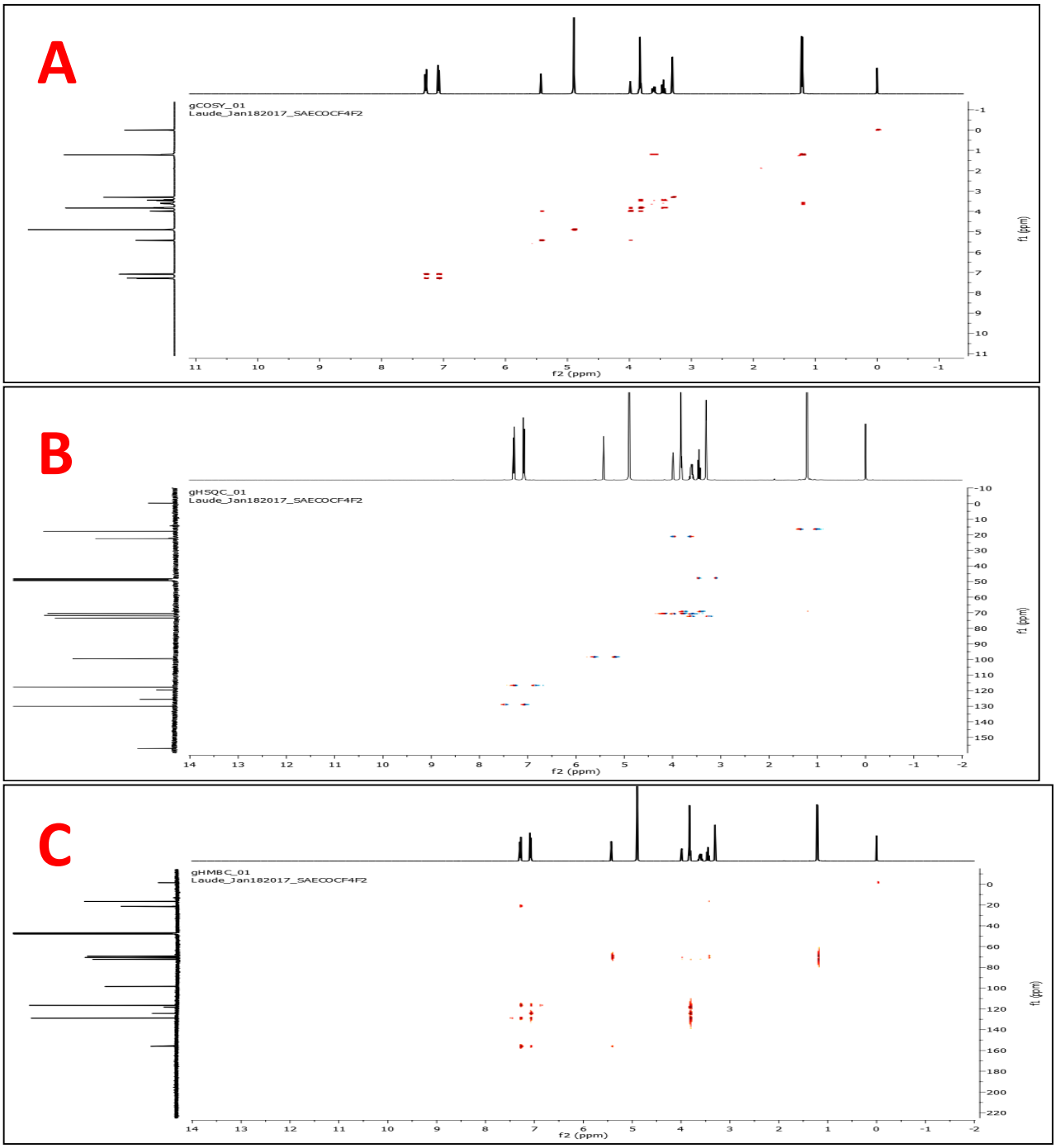

SI Figure 8D: 2D NMR of SAE-C-OCF4-F2 (niazirin). A. COSY B. HSQC C. HMBC. Chemical shifts were recorded at 500 MHz with CD_3OD as solvent. Acquired from UP Diliman.

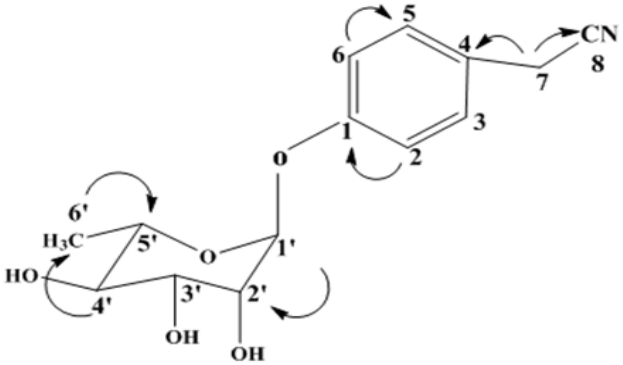

SI Figure 9: Structure of SAE-C-OCF4-F2 (niazirin). Arrows represent important HSQC and HMBC correlations

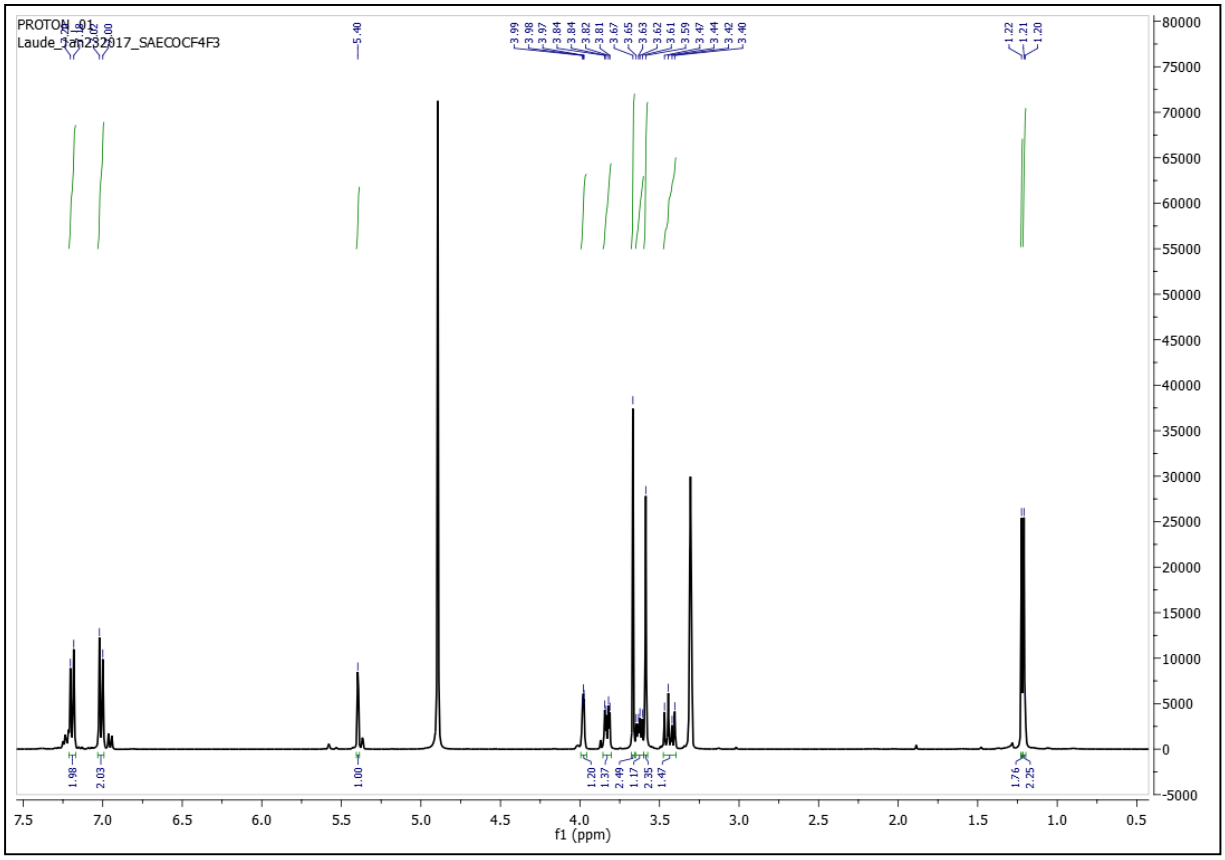

SI Figure 10A: ^{1}H-NMR spectral data of SAE-C-OCF4-F3. Chemical shifts were recorded at 500 MHz with CD_3OD as solvent. Acquired from UP Diliman.

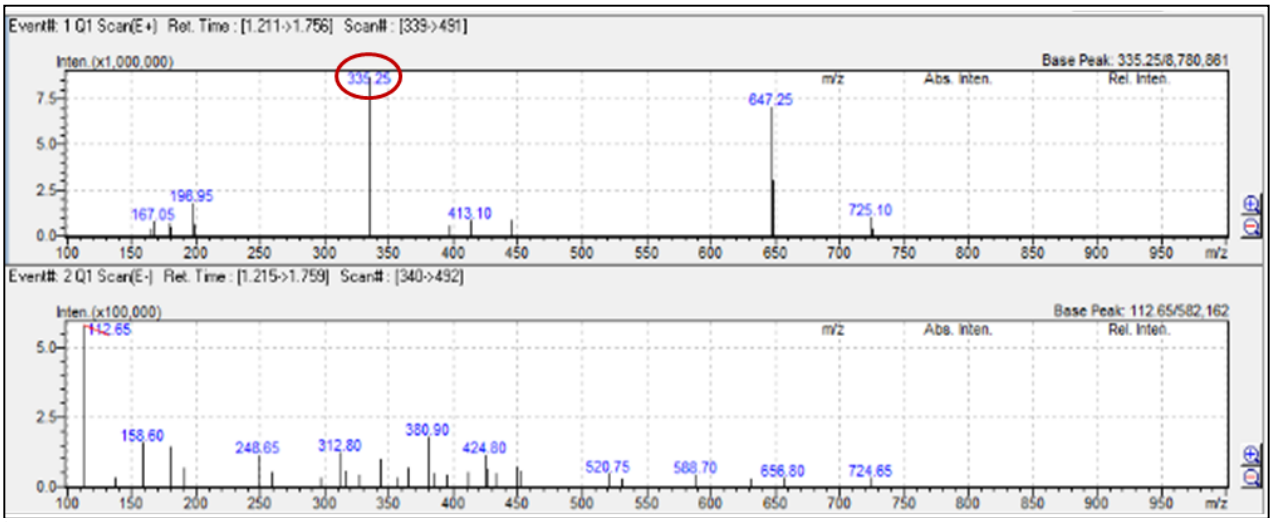

SI Figure 10B: Low resolution ESI-MS data acquired for SAE-C-OCF4-F3. Positive ionization mode (top) and negative ionization mode (bottom). Acquired from MSI, UP Diliman.

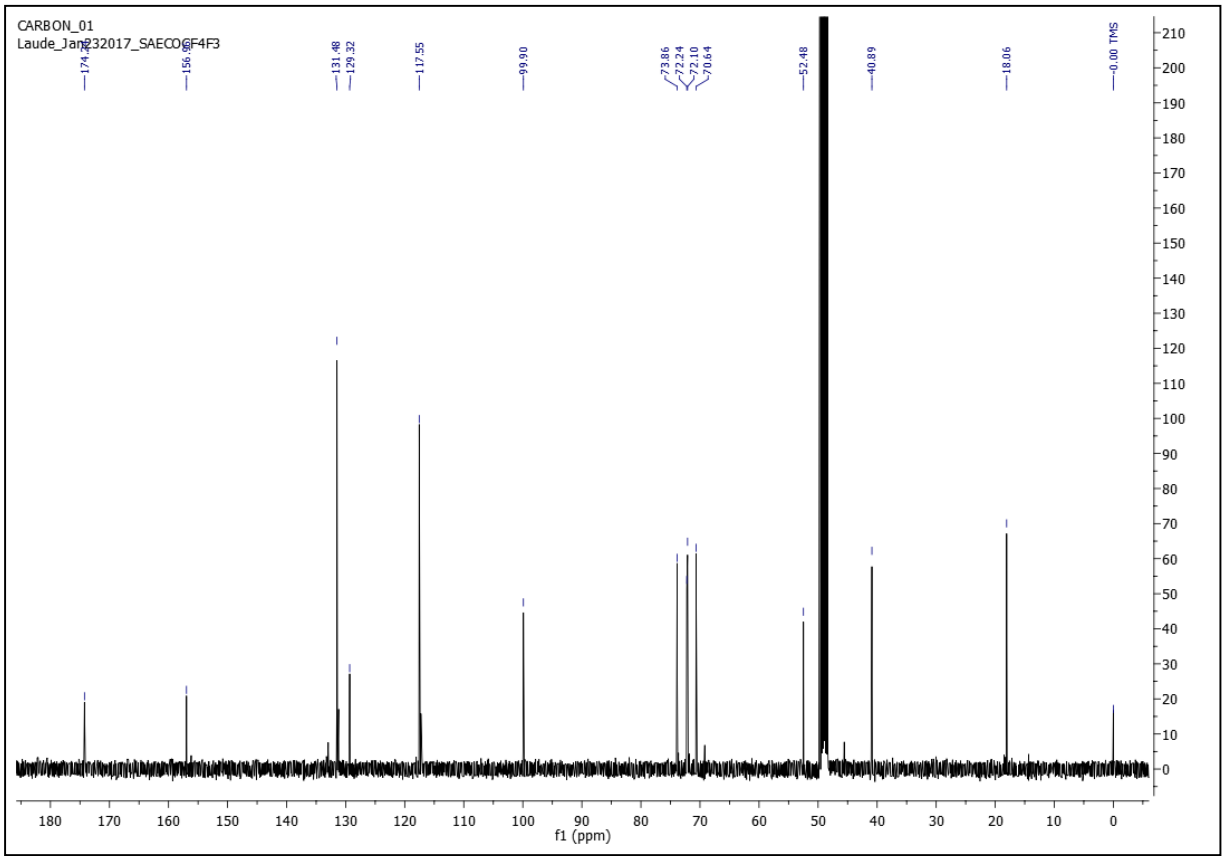

SI Figure 10C: ^{13}C-NMR of SAE-C-OCF4-F3. Chemical shifts were recorded at 500 MHz with CD_3OD as solvent. Acquired from UP Diliman.

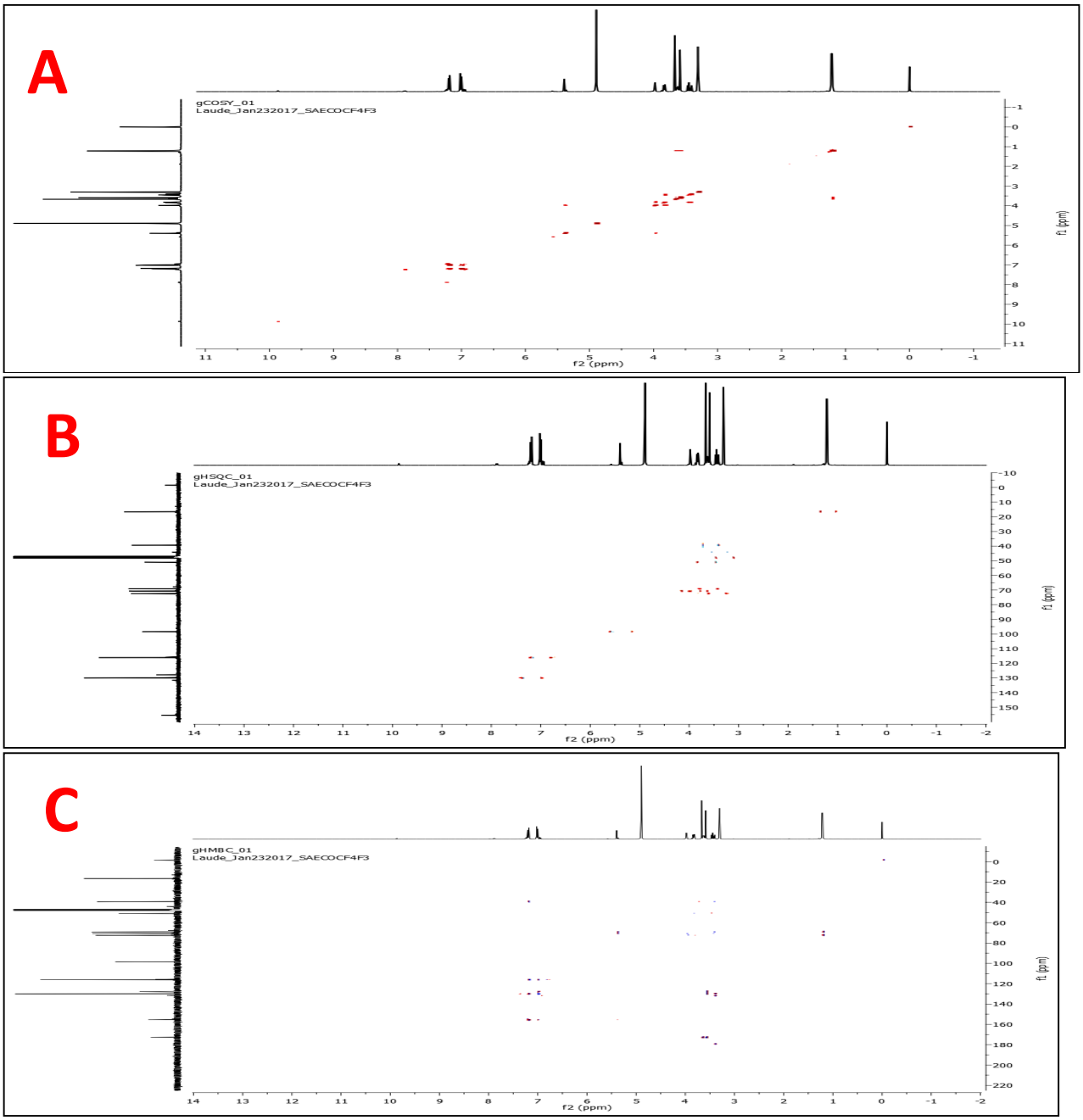

SI Figure 10D: 2D NMR of SAE-C-OCF4-F3. A. COSY B. HSQC C. HMBC. Chemical shifts were recorded at 500 MHz with CD_3OD as solvent. Acquired from UP Diliman.

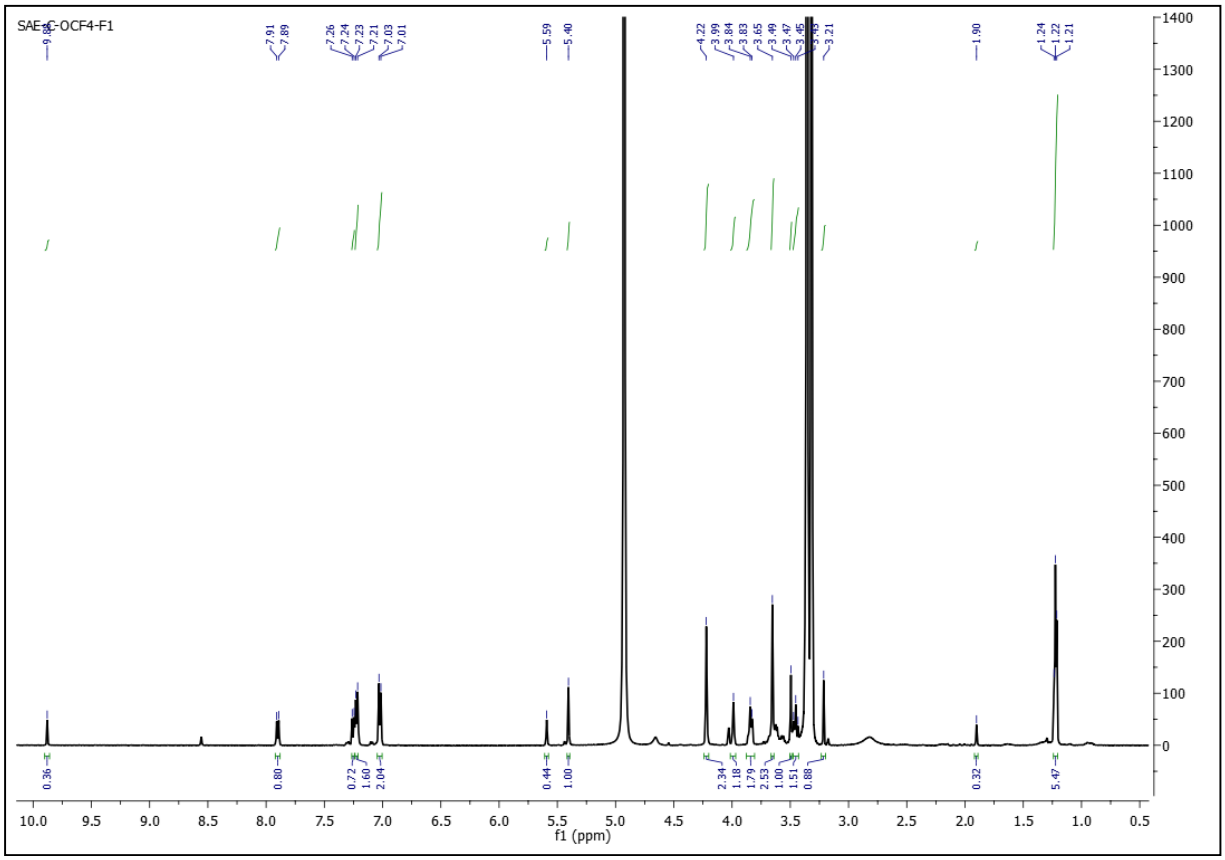

SI Figure 11A: ^{1}H-NMR spectral data of SAE-C-OCF4-F1. Chemical shifts were recorded at 500 MHz with CD_3OD as solvent. Acquired from UP Diliman.

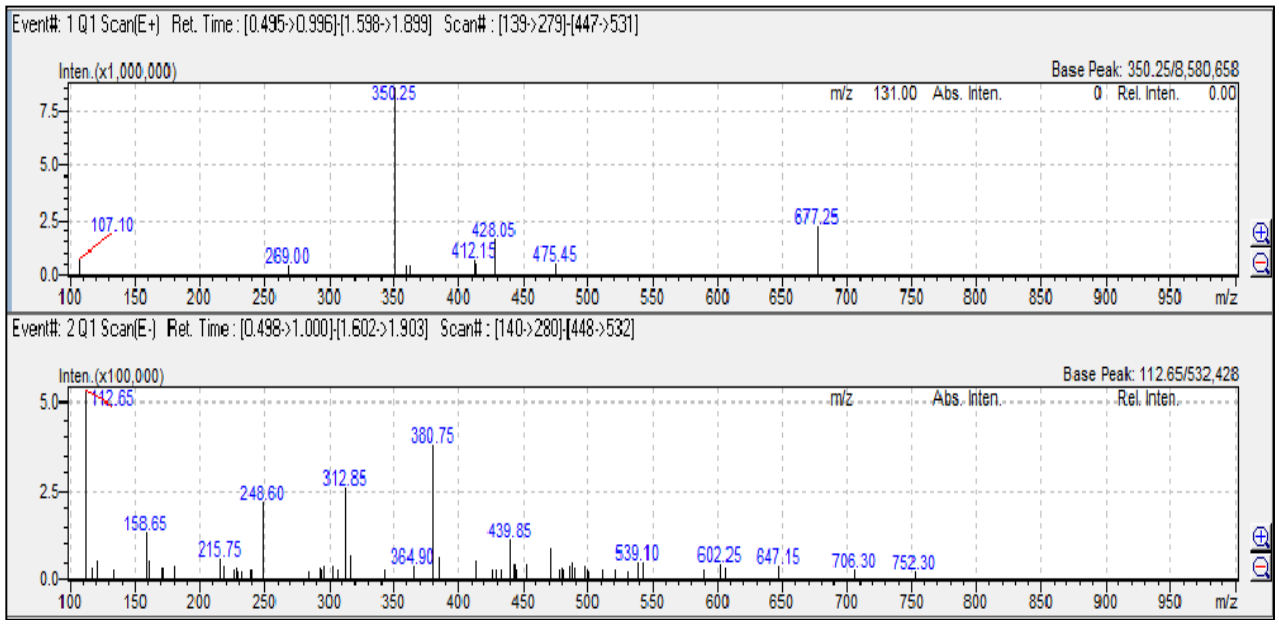

SI Figure 11B: Low resolution ESI-MS data acquired for SAE-C-OCF4-F1. Positive ionization mode (top) and negative ionization mode (bottom). Acquired from MSI, UP Diliman.

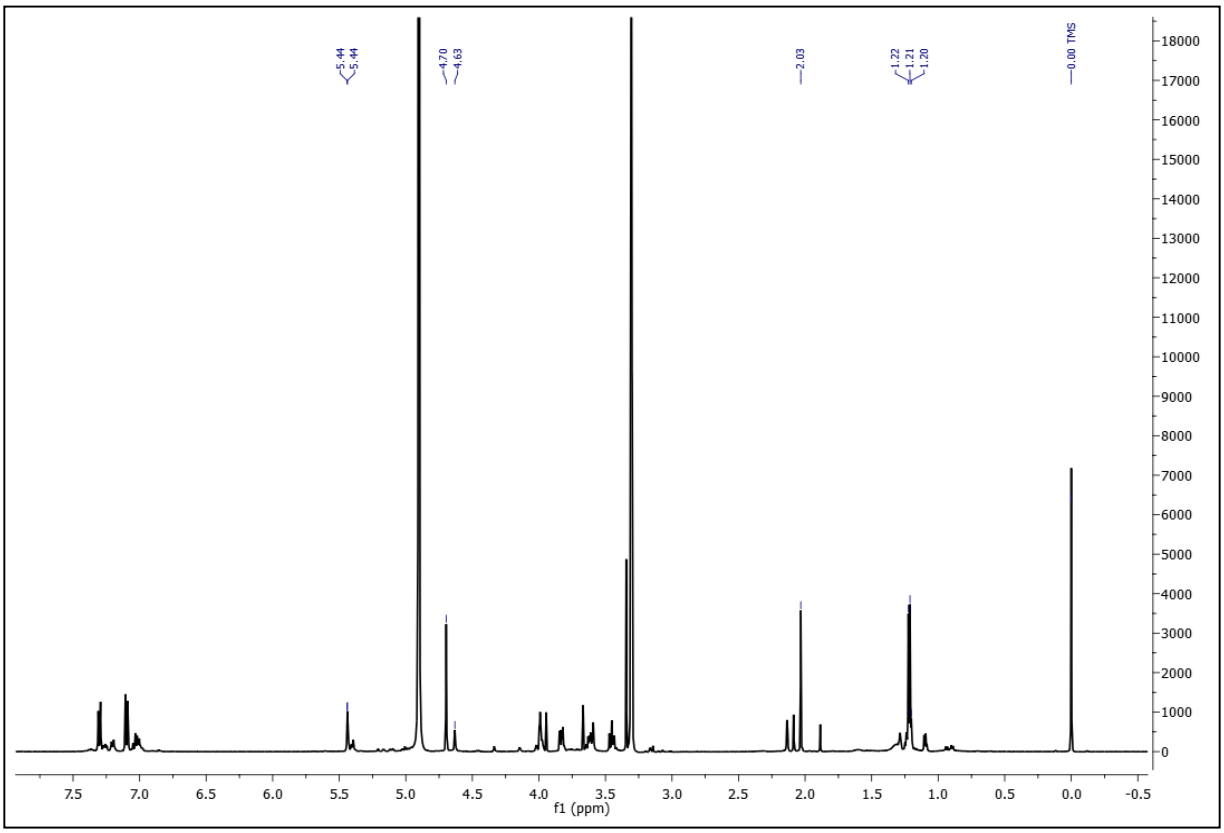

SI Figure 12: ^{1}H-NMR spectral data of SAE-C-OCF4-F6. Chemical shifts were recorded at 500 MHz with CD_3OD as solvent. Acquired from UP Diliman.

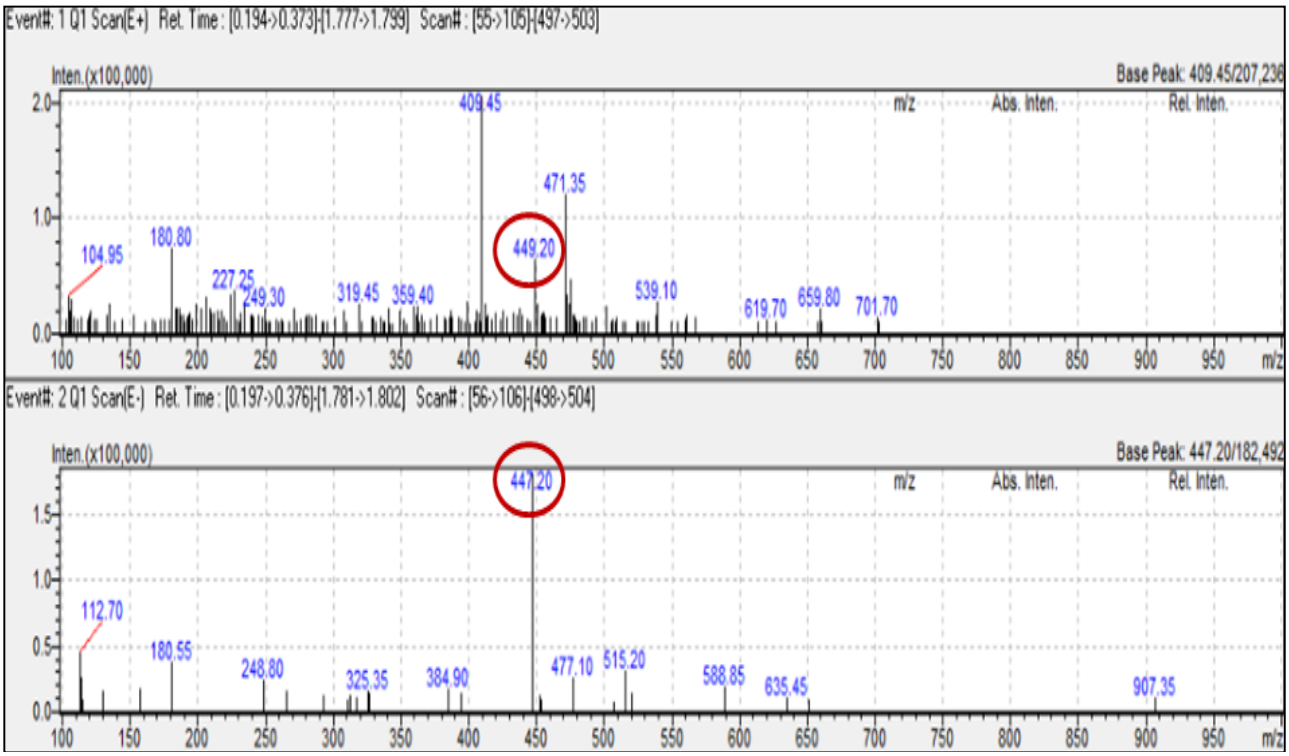

SI Figure 13: Low resolution ESI-MS data acquired for ULOE-OCF10-F1. Positive ionization mode (top) and negative ionization mode (bottom). Acquired from MSI, UP Diliman.

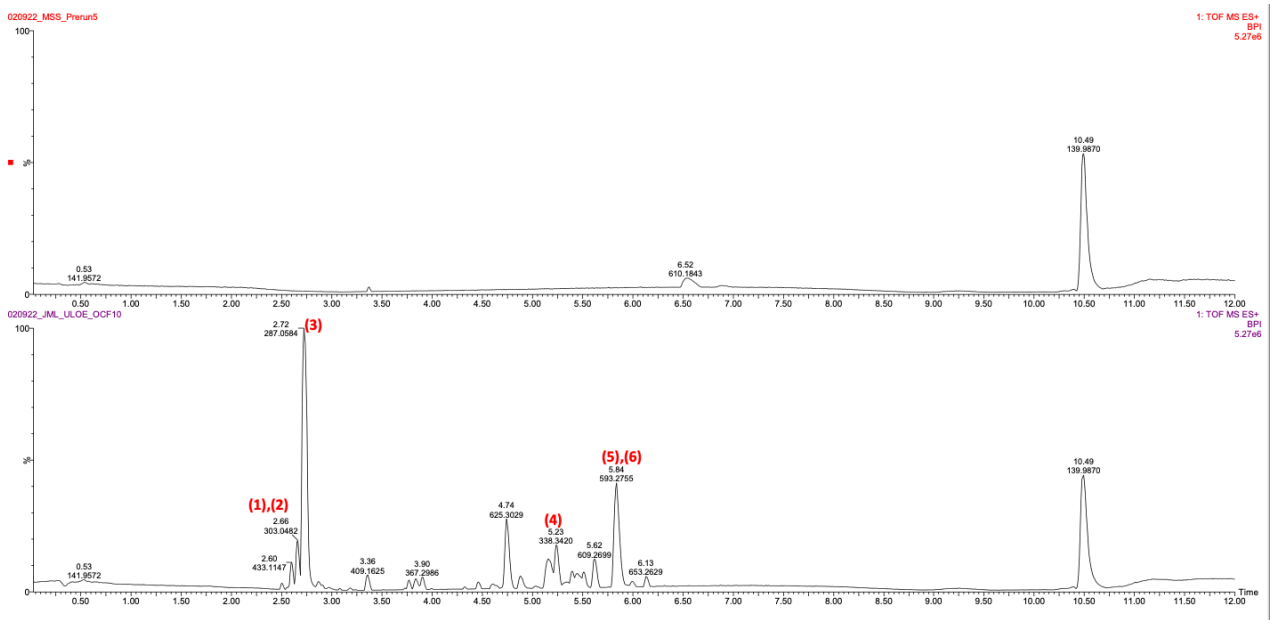

SI Figure 14: Mass spectra of ULOE-OCF10. Mass spectrometry was performed using UPLC-MS (Waters) in ESI positive mode.

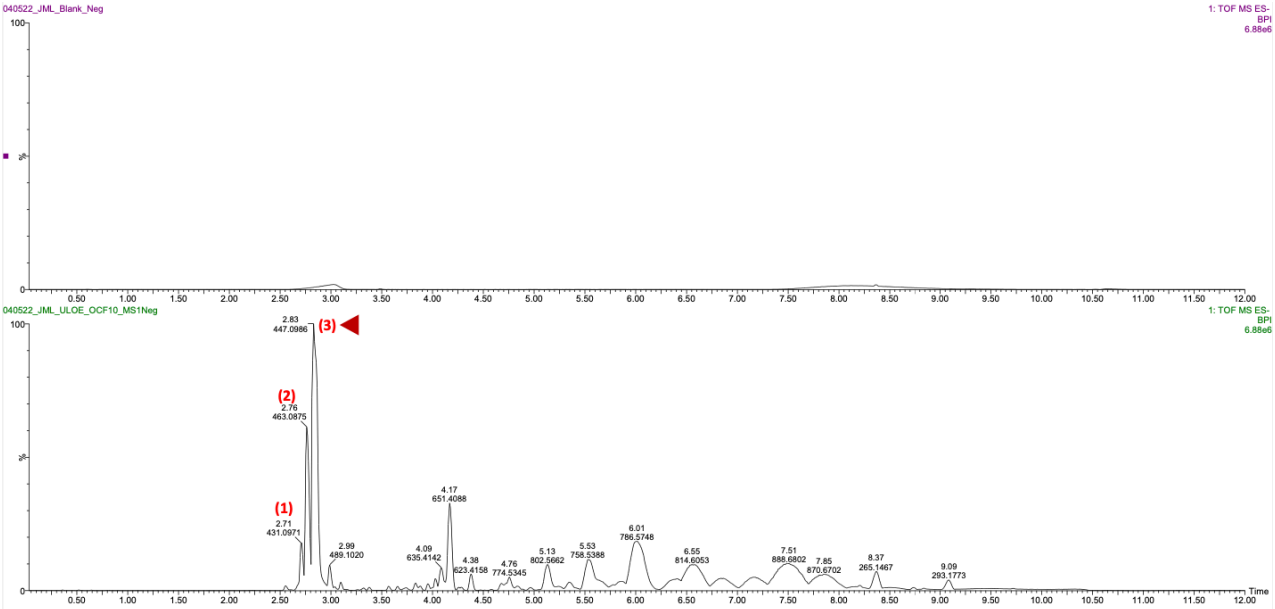

SI Figure 15: Mass spectra of ULOE-OCF10. Mass spectrometry was performed using UPLC-MS (Waters) in ESI negative mode.

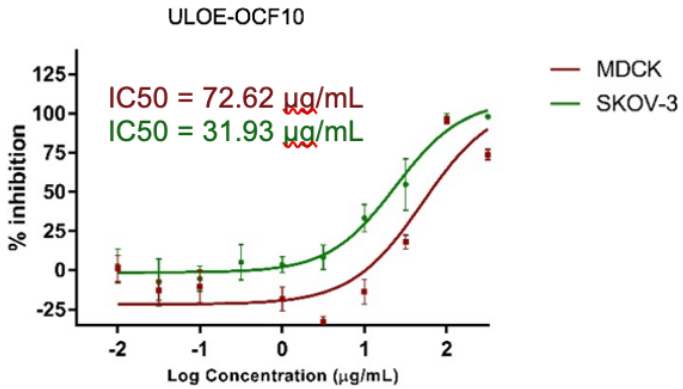

SI Figure 16: Dose-response curve ULOE OCF10 on MDCK and SKOV-3. Cells were treated with the compounds for 72 hours and the cytotoxicity was determined using MTT assay. Each point represents mean ± sd of four replicates performed in at least two independent trials. Cells used were less than passage 20.

SI Table 1: Culture conditions of cells used for assay. All cells used were below passage 20.

Normal Cell Lines	Seeding Densities in 96-Well Plate (cells/well)	Culture Conditions
human breast adenocarcinoma (MCF-7)	$2x10^4$	Minimum essential medium (MEM) with Earle's salts supplemented with 10% v/v fetal bovine serum (FBS), 1% v/v penicillin-streptomycin, 0.1 mM non-essential amino acids (Sigma), 2 mM L-glutamine, 0.01 mM sodium pyruvate, 0.2% w/v sodium bicarbonate, and 10 µg/ml human insulin (Sigma)
human ovary adenocarcinoma (SKOV-3)	$1x10^3$	McCoy's 5a medium with L-glutamine (Sigma) supplemented with 10% v/v FBS, 1% v/v pen-strep and 0.225% w/v sodium bicarbonate
human colorectal carcinoma (HCT 116)	$1x10^4$	McCoy's 5a medium with L-glutamine (Sigma) supplemented with 10% v/v FBS, 1% v/v pen-strep and 0.225% w/v sodium bicarbonate
human non-small cell lung carcinoma (A549)	$7.5x10^3$	D-MEM/F12 medium with L-glutamine supplemented with 10% v/v FBS, 1% v/v pen-strep and 0.15% w/v sodium bicarbonate
Cancer Cell Lines		
normal dog kidney (MDCK)	$2x10^4$	DMEM low glucose medium with L-glutamine (ThermoFisher) supplemented with 10% v/v FBS, 1% v/v pen-strep and 0.15% w/v sodium bicarbonate
normal human proximal tubular kidney (HK-2)	$7.5x10^3$	D-MEM/F12 medium with L-glutamine supplemented with 10% v/v FBS, 1% v/v pen-strep and 0.15% w/v sodium bicarbonate
African green monkey kidney (Vero)	$1x10^4$	Minimum essential medium (MEM) with Earle's salts supplemented with 10% v/v fetal bovine serum (FBS), 1% v/v penicillin-streptomycin, 0.1 mM non-essential amino acids (Sigma), 2 mM L-glutamine, 0.01 mM sodium pyruvate and 0.2% w/v sodium bicarbonate
human hepatocellular carcinoma (HepG2)	$1x10^4$	Eagle's Minimum Essential Medium (EMEM) with L-glutamine and HEPES supplemented with 10% v/v FBS, 1% v/v pen-strep and 0.15 % sodium bicarbonate

SI Table 2: ^{1}HNMR Spectroscopic Data for SAE-C-OCF4-F4 (niazinin) and SAE-C-OCF4-F5 (niazimicin) in CD_3OD.

Assignment	Compound	
	SAE-C-OCF4-F4 (niazinin) δ_H,multiplicity[a]	SAE-C-OCF4-F5 (niazimicin) δ_H,multiplicity[b]
H-2,-6	7.03, d	7.01, d
H-3,-5	7.26, d	7.24, d
H-7	4.64, s	4.63, s
H-1'	5.41,bs	5.40,bs
H-2'	3.99, m	3.98, m
H-3'	3.84, dd	3.82, dd
H-4'	3.45, m	3.44, m
H-5'	3.63, m	3.62, m
H-6'	1.22, d	1.21, d
OCH_3	3.95, s	-
$OC\mathbf{H_2}CH_3$	-	4.47, m
$OCH_2C\mathbf{H_3}$	-	1.29, m

[a]600 MHz
[b]500 MHz

SI Table 3: NMR spectroscopic data for SAE-C-OCF4-F2 (niazirin) in CD_3OD.

Assignment	δ ^{13}C[a]	δ ^{1}H[b]	COSY[b]
1	157.2	-	-
2,6	117.8	7.08, d	7.29
3,5	130.1	7.29, d	7.08
4	125.5	-	-
7	22.5	3.83, s	7.29
8	119.6	-	-
1'	99.5	5.43,bs	3.98
2'	71.7	3.98, bs	3.82, 5.43
3'	71.9	3.82, m	3.45, 3.82
4'	73.5	3.45, m	3.62, 3.82
5'	70.4	3.61, m	1.21, 3.45
6'	17.8	1.21, d	3.61

[a]125 MHz
[b]500 MHz

SI Table 4: ^{1}H-NMR and ^{13}C NMR Chemical Shifts for SAE-C-OCF4-F3 in CD_3OD.

Assignment	δ ^{13}C	δ ^{1}H	COSY	HMBC
1	157.0			
2,6	117.6	7.00, d	7.20	129.3
				131.5
				157
				40.9
3,5	131.5	7.20, d	7.00	131.5
				157.0
				117.6
4	129.3	-		
1'	99.9	5.40, bs	3.98	70.6
2'	72.1	3.98, bs	3.83, 5.40	72.4
3'	72.4	3.83, m	3.44, 3.98	
4'	73.9	3.44, m	3.83	70.6
5'	70.6	3.61, m	1.20	
6'	18.1			
Unassigned	40.9	3.59, s (CH_2)	1.21	
	52.5	3.67, s (CH_2)	1.21	
		1.21, s (CH_2)	1.21, 3.45	
		1.22, s (CH_2)		
	174.2			

Chemical shifts were recorded at 500 MHz (data from UP Diliman)

SI Table 5: ^{1}H-NMR and ^{13}C NMR Chemical Shifts for SAE-C-OCF4-F1 in CD_3OD

δ_H, ppm, multiplicity	Number of Protons	Type of Proton
7.20, d	2	Aromatic
7.00, d	2	Aromatic
5.40, s	1	anomeric
4.22, s	2	benzylic
3.98, bs	1	sugar-H
3.82, d	2	-
3.65, s	3	OCH_3
3.49, s	1	sugar-H
3.45, t	2	sugar-H
3.21, s	1	sugar-H
1.21,t	5?	sugar methyl

SI Table 6: Compounds identified by mass spectrometry in ULOE-OCF10. Mass spectrometry was performed using UPLC-MS (Waters) in ESI positive mode.

Peak No.	Putative ID	Cosine Score	Ion adduct	Monoisotopic mass, Da	Experimental mass, Da	Mass error, ppm
1	Quercetin-3-O-hexoside***	0.97	[M+H]+	464.09547607	465.1011	4.74
2	Quercetin***	0.95	[M+H]+	302.04265265	303.0518	4.38
3	Kaempferol	0.97	[M+H]+	286.04773803	287.0584	9.92*
4	13-docosenamide	0.78	[M+H]+	337.334464995	338.3420	0.86
5	GalCer(d18:2/20:1)**	0.93	[M+H]+	751.59621854	752.6034	0.86
6	Pheophorbide A **	0.95	[M+H]+	592.26857026	593.2755	1.51

* Initially not reported due to high mass error

** Co-elutes in the chrom at RT= 5.84 min. MassLynx only reports highest intensity mass per peak in the chrom.

***Co-elutes in the chrom at RT=2.66 min.

SI Table 7: Compounds identified by mass spectrometry in ULOE-OCF10. Mass spectrometry was performed using UPLC-MS (Waters) in ESI negative mode.

Peak No.	Putative ID	Cosine Score	Ion adduct	Monoisotopic mass, Da	Experimental mass, Da	Mass error, ppm
1	Vitexin	0.96	[M-H]-	432.10564683	431.0971	1.67
2	Isoquercitrin	0.94	[M-H]-	464.09547607	463.0875	0.33
3	Kaempferol-3-O-glucoside	0.98	[M-H]-	447.09273642	447.0986	3.94

SI Table 8: Cytotoxicity of the HPLC fractions from the open column fraction 4 of the chloroform partition of ethanolic seed extract (SAE-C-OCF4-Fs) against cancer cells[a] and normal kidney cells[a].

SAE-C-OCF4-Fs	A549 (lung)		HCT 116 (colon)		SKOV-3 (ovary)		MCF-7 (breast)		Vero (normal)	
	% Inhibition									
	50 µg/mL	5 µg/mL	50 µg/mL	5 µg/mL	50 µg/mL	5 µg/mL	50 µg/mL	5 µg/mL	50 µg/mL	5 µg/mL
F1	84.8 ± 1.4	13.5 ± 3.4	5.3 ± 7.3	13.5 ± 3.4	3.4 ± 3.9	14.4 ± 4.6	19.7 ± 6.0	15.1 ± 1.4	31.6 ± 3.9	21.4 ± 3.8
F2	11.7 ± 5.9	10.6 ± 2.6	2.3 ± 3.7	10.6 ± 2.6	11.0 ± 8.0	12.7 ± 2.5	14.5 ± 4.7	16.9 ± 0.8	25.6 ± 1.9	4.3 ± 3.4
F3	10.7 ± 7.1	1.2 ± 4.2	0.0 ± 3.3	1.2 ± 4.2	4.7 ± 2.4	6.4 ± 9.1	21.3 ± 3.4	27.7 ± 2.2	22.4 ± 1.9	9.5 ± 3.5
F4	9.0 ± 7.5	0.3 ± 1.9	2.7 ± 3.2	0.3 ± 1.9	9.2 ± 6.0	7.2 ± 5.3	30.8 ± 4.6	29.2 ± 3.6	16.2 ± 2.0	0.0 ± 7.5
F5	10.0 ± 4.1	0.0 ± 5.3	5.5 ± 1.5	0.0 ± 5.3	20.1 ± 4.4	34.7 ± 0.5	25.1 ± 2.4	26.4 ± 3.4	20.3 ± 2.1	4.0 ± 3.8
F6	24.8 ± 7.4	0.0 ± 2.9	80.4 ± 9.4	0.0 ± 2.9	73.1 ± 6.0	0.1 ± 5.6	74.3 ± 8.7	25.5 ± 5.6	45.9 ± 4.9	4.4 ± 5.5
Dox*	93.7 ± 0.7	17.2 ± 7.1	93.2 ± 8.9	28.3 ± 1.8	89.2 ± 1.0	4.4 ± 5.0	85.4 ± 5.8	8.2 ± 7.1	83.3 ± 7.9	1.6 ± 5.9

[a]All cells used in the assays were less than passage 20.
*Doxorubicin (Dox) was used as a positive control. Concentrations of Dox used for the assays were 0.54 µg/mL (1 µM) and 0.054 µg/mL (0.1 µM). These concentrations were based on the potencies of doxorubicin against the cell lines indicated.

cytotoxic (> 60% inhibition)

slightly cytotoxic (40-60% inhibition)

SI Table 9: Cytotoxicity of the upscale open column fractions from the ethanolic oven dried leaf extract (ULOE) against cancer cells[a] and normal kidney cells[a].

ULOE	MCF-7 (breast)		A549 (lung)		SKOV-3 (ovary)		MDCK (normal)	
	% inhibition							
	50 µg/mL	5 µg/mL	50 µg/mL	5 µg/mL	50 µg/mL	5 µg/mL	50 µg/mL	5 µg/mL
OCF1	13.1 ± 18.2	4.8 ± 4.0	24.1 ± 1.0	-0.15 ± 9.6	13.5 ± 8.1	10.2 ± 8.6	9.1 ± 1.2	-8.6 ± 9.9
OCF2	7.3 ± 18.0	3.5 ± 8.3	0.9 ± 8.5	6.82 ± 9.7	-38.2 ± 8.5	21.5 ± 9.6	-7.3 ± 8.7	-2.0 ± 8.7
OCF3	63.7 ± 5.5	10.8 ± 3.9	47.3 ± 7.9	-13.01 ± 7.9	28.9 ± 2.6	10.2 ± 3.4	43.1 ± 5.5	-4.3 ± 3.6
OCF4	83.7 ± 4.3	-6.9 ± 3.6	95.1 ± 2.8	4.63 ± 4.0	78.8 ± 3.9	16.8 ± 0.0	75.9 ± 7.2	-4.2 ± 6.6
OCF5	73.9 ± 10.9	6.4 ± 6.5	29.2 ± 2.2	-3.31 ± 9.9	45.6 ± 6.7	25.5 ± 5.9	66.4 ± 10.5	5.5 ± 6.4
OCF6	58.1 ± 4.3	15.3 ± 3.9	76.8 ± 6.1	12.88 ± 9.3	68.2 ± 5.5	36.8 ± 9.4	84.2 ± 10.0	0.0 ± 7.6
OCF7	95.7 ± 2.6	13.9 ± 4.9	96.8 ± 2.0	5.77 ± 8.1	94.8 ± 4.7	44.9 ± 9.0	92.1 ± 5.0	-13.1 ± 1.1
OCF8	78.0 ± 11.0	24.9 ± 2.8	99.1 ± 0.7	0.07 ± 3.2	95.6 ± 4.6	29.3 ± 7.0	88.5 ± 7.9	-1.4 ± 9.4
OCF9	74.8 ± 4.4	11.8 ± 6.0	51.1 ± 5.0	38.43 ± 9.6	56.4 ± 4.7	45.4 ± 5.7	16.8 ± 7.1	4.5 ± 13.1
OCF10	34.5 ± 7.4	15.0 ± 1.5	52.6 ± 8.3	20.47 ± 0.7	69.1 ± 3.9	23.3 ± 7.3	27.5 ± 0.0	4.6 ± 8.1
OCF11	37.0 ± 6.1	6.0 ± 5.1	-27.4 ± 5.4	-15.16 ± 8.9	-5.7 ± 9.8	-8.6 ± 6.1	-15.6 ± 6.2	-10.9 ± 3.1
OCF12	-39.4 ± 3.1	-33.0 ± 6.8	-32.9 ± 3.6	-14.5 ± 5.6	-2.7 ± 3.8	-0.1 ± 2.2	-12.4 ± 7.4	-9.3 ± 1.0
OCF13	-43.6 ± 5.4	-34.3 ± 8.9	-37.8 ± 9.5	-7.83 ±3.9	-4.5 ± 3.9	-14.6 ± 5.5	-15.4 ± 7.7	-16.9 ± 5.1
Dox*	99.5 ± 0.5	57.0 ± 2.0	97.6 ± 0.2	16.2 ± 5.6	89.9 ± 3.1	40.6 ± 8.9	85.0 ± 4.1	26.7 ± 3.3

[a]All cells used in the assays were less than passage 20.
*Doxorubicin (Dox) was used as a positive control. Concentrations of Dox used for the assays were 0.54 µg/mL (1 µM) and 0.054 µg/mL (0.1 µM). These concentrations were based on the potencies of doxorubicin against the cell lines indicated.

cytotoxic (> 60% inhibition)

slightly cytotoxic (40-60% inhibition)

SI Table 10: Vascularity scores observed in chorioallantoic membranes (CAMs) of eggs that were untreated, and treated with DMSO, endostatin, and priority HPLC Fs from S.A.E-C-OCF4 and S.A.E-H-OCF9, and IMLAE OCF4 based on CAM scoring guide by Burdick et al. 2003. (High dose, HD = 25 µg; and low dose, LD = 2.5 µg)

Samples	Vascular Damage	Interpretation
Untreated	0	No damage
DMSO	0	No damage
Endostatin (HD)	0	No damage
Endostatin (LD)	1.00	Ghost vessels
IMLAE HE5:3.OCF 4	3.75	26%-50% bleeding
IMLAE. HE5:3.OCF 4 HPLC frxn 3	2.67	25% bleeding
S.A.E-C-OCF4-HPLC F6 (HD)	5.00	51%-75% bleeding
S.A.E-C-OCF4-HPLC F6 (LD)	2.75	25% bleeding
S.A.E-H-OCF9-HPLC F7 (HD)	1.67	Increased blood flow
S.A.E-H-OCF9-HPLC F7 (LD)	1.67	Increased blood flow

SI Table 11: Fold change ARE activation of LNCaP and MDA-MB-231 cells treated with extracts from the leaves and seeds in RLU. Data are normalized to solvent control and to cell viability from MTT assay. Assay was done in triplicate.

Name/ Fr #		10 mg/mL (volug/mle; uL)	MTT (% viability)-LNCap			ARE activation/LNCap (normalized)			MTT (% viability)-MDA231			ARE inhibition (normalized)-MDA231		
			100 ug/ml	10 ug/ml	1 ug/ml	100 ug/ml	10 ug/ml	1 ug/ml	100 ug/ml	10 ug/ml	1 ug/ml	100 ug/ml	10 ug/ml	1 ug/ml
1	LAE	120	0.811	0.999	1.037	2.020	0.919	0.554	0.239	0.855	0.876	0.255	1.295	0.978
2	LAE-HE5:3	110	0.621	1.109	1.091	10.574	0.655	0.622	0.112	0.624	0.889	0.002	1.641	0.985
3	LAE-HE1:1	120	0.782	1.077	1.038	3.818	2.169	0.743	0.137	0.688	0.947	0.008	1.412	1.138
4	LAE-HE2:6	80	1.005	1.135	1.048	7.912	1.831	1.270	0.212	0.822	1.001	0.040	1.366	1.011
5	LAE-HE5:3-OCF1–2	110	0.834	1.006	1.020	4.115	1.108	1.703	0.080	0.641	0.966	0.002	3.450	0.930
6	LAE-HE5:3-OCF3	160	0.927	1.111	1.023	1.230	1.520	0.784	0.244	0.707	1.036	0.236	0.476	0.962
7	LAE-HE5:3-OCF4–6	120	0.893	1.040	1.093	2.264	1.088	0.405	0.263	0.804	0.940	0.032	1.166	0.933
8	LAE-HE5:3-OCF8	190	0.848	1.019	1.037	7.507	1.142	4.615	0.155	0.833	0.874	0.029	1.399	0.987
9	LAE-HE1:1-OCF3–5	100	0.941	1.082	1.041	8.189	0.689	2.400	0.337	0.389	0.884	0.091	1.742	1.164
10	LAE-HE1:1-OCF6	100	1.355	1.265	1.058	0.547	0.905	1.533	0.235	0.246	0.851	0.013	1.975	1.415
11	LAE-HE1:1-OCF8	150	1.352	1.174	1.023	0.453	1.236	2.867	0.358	0.365	0.892	1.548	1.445	1.311
12	LOE	120	1.288	1.207	1.030	0.507	1.108	1.733	0.252	0.276	0.871	0.092	1.207	1.452
13	SAE-C	1030	1.302	1.125	1.046	0.804	1.595	3.467	0.751	0.699	1.021	2.094	1.227	1.198
14	SAE-H	620	1.289	1.105	1.075	1.669	0.892	1.067	0.404	0.536	0.973	2.285	1.216	1.180
15	SAE-E	1750	1.238	1.084	1.073	0.345	0.270	1.867	0.999	0.999	1.021	1.265	1.118	1.149
16	SAE-H-OCF3a	120	1.170	1.028	1.123	0.554	0.230	0.867	0.502	0.507	0.819	3.097	1.651	1.144
17	SAE-H-OCF3b	80	0.997	1.188	1.087	1.486	1.333	0.867	0.725	1.065	1.022	3.651	1.555	0.912
18	SAE-H-OCF4	150	0.843	1.145	1.047	3.716	2.267	2.600	0.398	0.899	1.004	2.471	1.379	1.094
19	SAE-H-OCF5	340	0.977	0.993	1.077	3.088	1.667	4.533	0.234	0.863	0.978	0.688	1.380	1.236
20	SAE-H-OCF6	120	0.906	1.070	1.056	2.730	2.400	3.000	0.724	0.952	1.037	2.753	1.372	0.990
21	SAE-C-OCF3	190	0.655	0.875	1.053	5.628	4.467	12.467	0.180	0.801	0.954	0.071	1.318	1.094
22	SAE-C-OCF4–5	930	0.956	1.050	1.059	6.588	2.133	3.800	0.550	0.955	0.980	2.461	1.281	1.033
23	SAE-E-OCF4	660	0.977	1.165	1.086	17.459	8.267	1.733	0.525	0.966	0.945	0.012	1.380	1.044
24	SAE-E-OCF5	160	0.689	1.206	1.174	7.885	6.467	1.733	0.110	0.835	0.938	0.005	1.094	0.944
25	LOE-OCF5–6	60	0.267	0.874	0.981	0.068	6.547	0.831	0.115	0.454	0.939	0.002	0.170	1.118
26	LOE-OCF10	50	1.017	0.935	1.026	14.865	1.419	0.432	0.011	0.786	1.001	0.004	2.407	1.086
27	SAE-C-OCF4–5-F4	70	1.177	0.951	1.051	3.800	1.867	2.800	0.914	0.966	0.982	2.033	1.383	1.207
28	SAE-C-OCF4–5-F2	140	1.074	0.968	1.000	2.200	1.867	1.433	0.939	0.977	0.945	1.458	1.103	1.119
29	SAE-C-OCF4–5-F3	60	0.979	1.025	0.916	2.800	1.278	1.800	0.905	0.976	0.941	1.361	1.012	1.059
30	LAE-HE5:3-OCF4–6-F2–4	30	1.305	1.035	1.064	1.333	1.600	1.044	0.903	0.916	0.959	1.565	1.168	1.156
Sulforaphane 10 uM						48.223								
Brusatol 125 nM									0.514			0.048		

SI Table 12: Summary of compounds from ethanolic seed extract SAE-C-OCF4, their bioactivities and concentration at which the bioactivity was observed

		Antiproliferation				
	Putative Compound Identity	Cancer Cells	Normal Cells	Apoptosis	Anti-migration	Anti-angiogenesis
Fraction	Cut-off value for activity	60%	60%		Migration index<1	*p<0.05, **p<0.01
SAE-C-OCF4-F1	Unidentified	50 µg/mL Lung (84.8%)				
SAE-C-OCF4-F2	Niazirin				5 µg/mL	25 µg/mL*
SAE-C-OCF4-F3	Unidentified				5 µg/mL	25 µg/mL**, 2.5 µg/mL *
SAE-C-OCF4-F4	Niazinin				5 µg/mL	
SAE-C-OCF4-F5	Niazimicin			50 µg/mL	5 µg/mL	25 µg/mL**, 2.5 µg/mL **
SAE-C-OCF4-F6	Niaziminin	50 µg/mL Colon (80.4%) Ovary (73.1%) Breast (74.3%)	50 µg/mL Vero (45.9%)	50 µg/mL		